Swansea University
Prifysgol Abertawe

Cronfa
Setting Research Free

**Cronfa - Swansea University Open Access Repository**

This is an author produced version of a paper published in:
*Composites Part B: Engineering*

Cronfa URL for this paper:
http://cronfa.swan.ac.uk/Record/cronfa46044

**Paper:**
Aria, A. & Friswell, M. (2018). A nonlocal finite element model for buckling and vibration of functionally graded nanobeams. *Composites Part B: Engineering*
http://dx.doi.org/10.1016/j.compositesb.2018.11.071

This item is brought to you by Swansea University. Any person downloading material is agreeing to abide by the terms of the repository licence. Copies of full text items may be used or reproduced in any format or medium, without prior permission for personal research or study, educational or non-commercial purposes only. The copyright for any work remains with the original author unless otherwise specified. The full-text must not be sold in any format or medium without the formal permission of the copyright holder.

Permission for multiple reproductions should be obtained from the original author.

Authors are personally responsible for adhering to copyright and publisher restrictions when uploading content to the repository.

http://www.swansea.ac.uk/library/researchsupport/ris-support/

# Accepted Manuscript

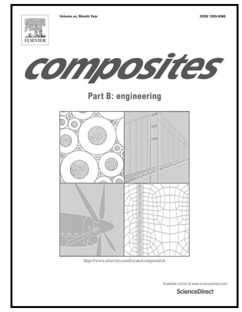


A nonlocal finite element model for buckling and vibration of functionally graded nanobeams

A. Imani Aria, M.I. Friswell

PII: S1359-8368(18)32983-4

DOI: https://doi.org/10.1016/j.compositesb.2018.11.071

Reference: JCOMB 6256

To appear in: *Composites Part B*

Received Date: 10 September 2018

Revised Date: 1 November 2018

Accepted Date: 15 November 2018

Please cite this article as: Aria AI, Friswell MI, A nonlocal finite element model for buckling and vibration of functionally graded nanobeams, *Composites Part B* (2018), doi: https://doi.org/10.1016/j.compositesb.2018.11.071.

This is a PDF file of an unedited manuscript that has been accepted for publication. As a service to our customers we are providing this early version of the manuscript. The manuscript will undergo copyediting, typesetting, and review of the resulting proof before it is published in its final form. Please note that during the production process errors may be discovered which could affect the content, and all legal disclaimers that apply to the journal pertain.

# A nonlocal finite element model for buckling and vibration of functionally graded nanobeams

A. Imani Aria[a], M. I. Friswell[b, 1]
[a]Tabriz University, Department of Mechanical Engineering, Tabriz, Iran.
[b]Swansea University, Bay Campus, Fabian Way, Swansea SA1 8EN, UK

## Abstract

In this paper, a nonlocal (strain-driven) finite element model is presented to examine the free vibration and buckling behaviour of functionally graded (FG) nanobeams on the basis of first-order shear deformation theory (FSDBT). The proposed beam element has five nodes and ten degrees of freedom. The material properties of the FG nanobeam are assumed to vary in the thickness direction according to the power-law form. The stretching-bending coupling effect is eliminated by employing the neutral axis concept. Governing equations are deduced with the aid of Hamilton's principle. Buckling loads and natural frequencies are calculated for different nonlocal coefficients, boundary conditions (BCs), power-law indices, and span-to-depth ratios. The accuracy of the proposed element is verified by comparing with available benchmark results in the literature.

Keywords: Functionally graded materials; Nonlocal elasticity theory; Finite element method; Free vibration; Buckling; First-order shear deformation theory.

## 1. Introduction

Many new materials and devices can be manufactured by nanotechnology techniques for a wide range of applications, such as cell manipulation [1], microsurgery [2], nanosensors, nanocomposites and smart systems and structures [3]. Investigation of micro/nano structural elements such as beams and plates at the micro/nano- length scale has gained the attention of many researchers, recently. Because of the high cost of atomic and molecular simulations, continuum models are commonly employed to study these elements where size effects are important in the simulations [4].

High order continuum theories to model micro/nano-scale structures have been used to capture the size effects of such structures considering the interactions of non-adjacent atoms and molecules. The most common continuum mechanics theory for modelling nanostructures is nonlocal elasticity. Nonlocal elasticity theory (strain-driven), which was developed by Eringen [5], models long range interactions between atoms. In accordance with Eringen's nonlocal model, the stress of a given point in a continuum body has interaction with strains at all points in that continuum body, not only those near the specific point. Later, Eringen [5] introduced a differential constitutive theory, and proved that for a particular type of kernel function the nonlocal integral constitutive relation could be transformed to differential form, which can be solved much easier, compared with the integral model. This differential formulation was used

[1] Corresponding author: Tel: +44 (0)1792 602969
E-mail address: m.i.friswell@swansea.ac.uk



ACCEPTED MANUSCRIPT

later in applications to bounded continuous structural models [6]. However, the fact that the constitutive boundary conditions on the stress naturally appear when working with bounded domains was neglected [7-10]. By adding the corresponding constitutive boundary conditions, an ill-posed problem is obtained. This happens because of the conflict between the constitutive and equilibrium conditions on the stress field. Hence, there is no solution for the continuous nonlocal elasto-static problem and this justifies the existence of the paradoxical results in literature [11-13]. This problem can be solved by employing a stress-driven model where the roles of stress and strain fields are interchanged [14]. Recently, some applications have been reported on the basis of the stress-driven model [15-19].

However, it should also be recognised that the nonlocal model in integral form is unable to model detailed local effects at boundaries, and hence there are always likely to be discrepancies between the actual and simulated bending moment at the boundary. Given that these discrepancies at the boundaries are always likely to be present whichever model used, here the differential form of the equations, or strain-driven model, is used [20]. Friswell et al. [21] proposed a finite element formulation for nonlocal elastic and viscoelastic foundations for Euler-Bernoulli beams. They studied the free vibrations of beams on nonlocal foundations and reported corresponding results for different kernel functions. Phadikar and Pradhan [22] presented a variational formulation and used finite element analysis to capture the size effects of nanobeams and nanoplates employing nonlocal elasticity theory. Murmu and Adhikari [23] introduced a nonlocal double-elastic beam model, and used it to analyse size effects on the free vibration of double-nanobeam systems. Mustapha and Zhong [24] studied the free vibration of an axially loaded single-walled carbon nanotube resting on a two parameter elastic foundation by employing the Bubnov–Galerkin method. Roque et al. [25] studied the mechanical behaviour of Timoshenko nanobeams in bending, buckling and free vibration using a meshless method. Thai [26] and Thai and Vo [27] used Eringen's nonlocal elasticity theory to introduce nonlocal shear deformation beam theory for bending, buckling and vibration of homogeneous materials. Lei et al. [28] employed velocity-dependent external damping to investigate the dynamic behaviour of damped nonlocal Timoshenko beams. Civalek and Demir [29] analysed buckling of microtubules on an elastic medium using finite element method and achieved critical buckling loads for various types of microtubules.

Functionally graded materials (FGMs) are composites, which possess variable microstructure that changes from one material to another with a specific gradient, with a corresponding variation in the effective material properties (i.e. shear modulus, material density and elasticity modulus). The FGMs take advantage of different characteristics of its component phases. For example, in a thermally dominant situation; the ceramic portion is employed to resist high temperature gradients because of its great thermal resistance properties, while the metal part provides suitable force endurance performance [30]. For specific functions and applications, the corresponding FGMs are designed in order to provide the optimum distribution of component materials. Moreover, FGMs have been intensely utilized in micro/nano devices, such as atomic force microscopes (AFMs) [31], electrically actuated actuators [32] and microswitches [33]. The free and forced vibration behaviour of graded micro and nanobeams have been studied by performing a range of numerical and analytical solutions. The following summarises the academic studies that have employed Eringen's nonlocal elasticity model to study vibration and buckling of nanobeams. Eltaher et al. [34] investigated the linear nonlocal free vibration of a Euler-Bernoulli FG nanobeams by employing finite element analysis. Uymaz [35] solved the free vibration problem of graded nanobeams for various beam theories by employing Navier's solution. Vibration behaviour of nonlocal FG beams was examined by Rahmani and Pedram [36]. They employed closed-form solutions to analyse the effects of length scale parameter, slenderness ratio and gradient index on natural frequencies. Nejad and Hadi [37] used the Generalized Differential Quadrature Method (GDQM) to analyse the nonlocal free vibration of bi-directional graded Euler-Bernoulli nanobeams. The nonlinear free vibration of a nonlocal FG Euler-Bernoulli nanobeam with nonlinear von Kármán strains was studied by Simsek et al. [38]. Niknam and Aghdam [39] investigated the large amplitude buckling and free vibration of nonlocal graded nanobeams embedded in elastic foundations exploiting He's variational method while accounting for the nonlinear von Kármán strains. El-Borgi et al. [40] employed the method of multiple scales and Galerkin's method to investigate the nonlocal nonlinear free and forced vibration behaviour of FG nanobeams embedded in a nonlinear elastic foundation. Thai et al. [41] utilized Eringen's elasticity theory to examine the postbuckling behaviour of functionally graded nanoplates. Eringen's strain-driven nonlocal integral formulation was employed by Baretta et al. [42] in order to investigate the size dependent bending response of Euler-Bernoulli nanobeams. Dastjerdi and Akgoz [43] studied the dynamic and static behaviours of FGM nanoplates by exploiting three-dimensional elasticity theory with the nonlocal theory of Eringen.

The finite element method (FEM) is one of the commonly employed numerical methods in analyses of nanostructures, although there are few developed finite elements to investigate FG nanobeams. On the basis of the classical beam theory, Eltaher et al. [34] proposed a two-noded, six degrees-of-freedom finite element to examine free vibration of FG nanobeams. They employed nonlocal elasticity theory in order to incorporate size effects. In a separate work, Eltaher et al. [44] studied the static and stability analysis of FG nanobeams based on Euler-Bernoulli beam theory (EBT), exploiting a two-noded beam element.

Finite element studies investigating FG nanobeams [34,44] that are reported in the literature, have employed a two-noded beam element with six degrees of freedom on the basis of EBT. A novel contribution of this study is to propose a five-noded nonlocal beam element with ten degrees of freedom considering shear displacements in addition to axial displacements. The present study develops an accurate finite element analysis in accordance with the first-order shear deformation theory (FSDBT) in the framework of Eringen's nonlocal elasticity theory for vibration and buckling analysis of functionally graded nanobeams, where material distribution is imposed as a through-thickness power-law variation. The weak form of equations and the corresponding boundary conditions are deduced using Hamilton's principle. The finite element has five nodes and ten degrees of freedom. The validity of the element is verified by comparing with benchmark results available in the literature for buckling loads and natural frequencies of functionally graded beams and homogenous nanobeams with different nonlocal coefficients, boundary conditions, power-law indices, and span-to-depth ratios.

# 2. Formulation

## 2.1 Functionally graded materials

For an FGM beam (Fig. 1), the material properties vary continuously in the z direction, and are assumed to take the form

$$P(z) = (P_1 - P_2)\left(\frac{z}{h} + \frac{1}{2}\right)^k + P_2 \tag{1}$$

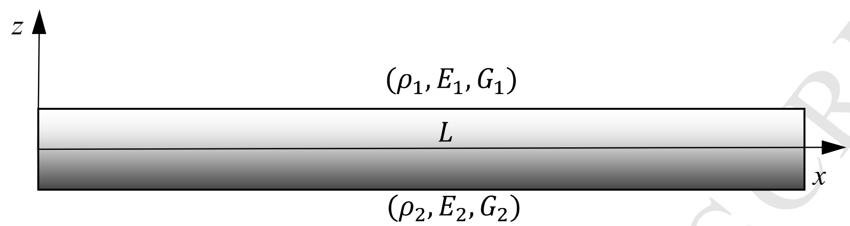


Fig.1 Geometry and coordinate system of a functionally graded beam.

where $k$ is the non-negative power-law exponent, and $P_1$ and $P_2$ are the related material properties of the ceramic and metal constituents. The Young's modulus, $E(z)$, shear modulus, $G(z)$, and material density, $\rho(z)$, may be defined based on this distribution function as

$$E(z) = (E_1 - E_2)\left(\frac{\bar{z}}{h} + \frac{1}{2}\right)^k + E_2 \tag{2}$$

$$G(z) = (G_1 - G_2)\left(\frac{\bar{z}}{h} + \frac{1}{2}\right)^k + G_2 \tag{3}$$

$$\rho(z) = (\rho_1 - \rho_2)\left(\frac{\bar{z}}{h} + \frac{1}{2}\right)^k + \rho_2 \tag{4}$$

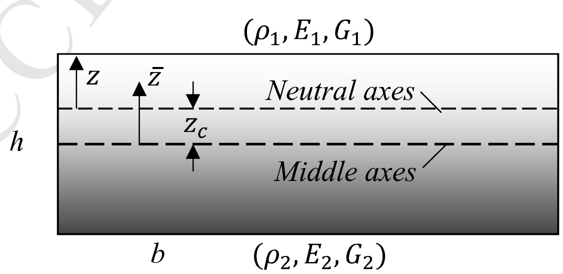


Fig.2 The position of the middle and neutral axis of FG beam.

In non-homogeneous beams, the variation of the elasticity modulus through the thickness is not symmetric with respect to the mid-plane. So, the neutral axis of the beam and the mid-plane do not coincide with each other. Thus, the position of the neutral axis has to be found and $z$ axis defined from the neutral axis (Fig. 2). The position of the neutral axis ($z_c$) can be calculated by [45-47]:

$$z_c = \frac{\int_A E(\bar{z})\bar{z}dA}{\int_A E(\bar{z})dA} \tag{5}$$

Based on the position of the neutral axis, the effective Young's modulus $E(z)$, the effective shear modulus $G(z)$, and the effective material density $\rho(z)$, are defined as

$$E(z) = (E_1 - E_2)\left(\frac{z}{h} + \frac{1}{2}\right)^k + E_2 \tag{6}$$

$$G(z) = (G_1 - G_2)\left(\frac{z}{h} + \frac{1}{2}\right)^k + G_2 \tag{7}$$

$$\rho(z) = (\rho_1 - \rho_2)\left(\frac{z}{h} + \frac{1}{2}\right)^k + \rho_2 \tag{8}$$

## 2.2 Nonlocal elasticity theory

Based on the nonlocal elasticity theory [5], the elastic strain field $\boldsymbol{\varepsilon^{el}}$ is the solution of a Fredholm integral equation. Hence, the stress $\boldsymbol{\sigma}$ is obtained by a convolution between the local feedback to the elastic strain and a scalar kernel dependent on a positive nonlocal parameter $\mu$. The stress at a point $\mathbf{x}$ in an elastic body, not only depends on the strain at that specific point, but also on the strain at all points in the continuum body. Hence, the nonlocal stress tensor is given by

$$\boldsymbol{\sigma} = \int_V \alpha_\mu(\boldsymbol{x} - \boldsymbol{x}').\boldsymbol{C}(\boldsymbol{x}').\boldsymbol{\varepsilon^{el}}(\boldsymbol{x}')dV \tag{9}$$

where $\alpha_\mu$ is the principal attenuation kernel function that determines the constitutive equations for the nonlocal effects at the reference point $\boldsymbol{x}$ produced by the local strain at the source $\boldsymbol{x'}$. $e_0 a$ denotes the nonlocal parameter that incorporates the nonlocal elastic stress field, where $e_0$ is a constant appropriate to each material and $a$ is an internal characteristic length, $\boldsymbol{C}$ is the fourth-order elasticity tensor, $\boldsymbol{\varepsilon}$ is the strain tensor and ":" denotes double-dot product of tensors.

Since the $\boldsymbol{\varepsilon^{el}}$ is the elastic strain, the model in Eq. (9), expresses the strain-driven nonlocal integral law [48, 49]. Consequently, the flexural nonlocal elastic law is shown based on an elastic curvature field $\phi^{el} \in \mathcal{H}$, which is square integrable on $[a, b]$, and having the local elastic flexural stiffness $K \in \mathcal{H}$.



ACCEPTED MANUSCRIPT

$$M(x) = \int_a^b \alpha_\mu(x - x').K(x').\phi^{el}(x')dx' \tag{10}$$

In the stress-driven model, proposed by Romano and Barretta [14], the roles of bending interaction and curvature fields are interchanged in comparison with the strain-driven model (Eq. (9)) and the following relation is obtained

$$\phi^{el}(x) = \int_a^b \alpha_\mu(x - x').K(x').M(x')dx' \tag{11}$$

Thus, the formulation of the stress-driven model is achieved by interchanging the roles of stress and strain fields with respect to the strain-driven model [14], giving

$$\boldsymbol{\varepsilon}^{\boldsymbol{el}} = \int_V \alpha_\mu(\boldsymbol{x} - \boldsymbol{x}').\boldsymbol{C}(\boldsymbol{x}').\boldsymbol{\sigma}(\boldsymbol{x}')dV \tag{12}$$

It is worth highlighting that these two laws (strain-driven and stress-driven) do not conflict with each other and result in different structural models.

In this paper, the differential law obtained from Eringen's strain-driven nonlocal integral convolution in Eq. (9), equipped with the bi-exponential averaging kernel, is employed

$$(1 - (e_0 a)^2 \nabla^2)\boldsymbol{\sigma} = \boldsymbol{C} : \boldsymbol{\varepsilon} \tag{13}$$

where $\nabla^2 = \frac{\partial^2}{\partial x^2} + \frac{\partial^2}{\partial y^2} + \frac{\partial^2}{\partial z^2}$ is the Laplacian operator.

For a beam type structure, by considering the nonlocal behavior in the thickness direction, the softening effect will depend on the span to depth ratio, in addition to the nonlocal parameter [50]. In this paper, the nonlocal effect in the thickness direction is ignored, and so the softening behavior is only dependent on the nonlocal parameter. Then, the nonlocal constitutive relation will take the form:

$$\sigma_{xx} - (e_0 a)^2 \frac{\partial^2 \sigma_{xx}}{\partial x^2} = E(z)\varepsilon_{xx} \tag{14}$$

$$\sigma_{xz} - (e_0 a)^2 \frac{\partial^2 \sigma_{xz}}{\partial x^2} = G(z)\gamma_{xz} \tag{15}$$

where $\sigma_{xx}$ is the axial normal stress, $\sigma_{xz}$ is the shear stress, $\varepsilon_{xx}$ is the axial strain and $\gamma_{xz}$ is the shear strain, $E(z)$ denotes the elasticity modulus and $G(z)$ denotes the shear modulus of the FGBs. Also, by letting $e_0 a = 0$, constitutive relation for the classical (local) theory is derived.

## 2.3 Timoshenko beam theory based on nonlocal elasticity



ACCEPTED MANUSCRIPT

The displacement field of a Timoshenko beam is given by

$$u_x(x,z,t) = u(x,t) - z\phi(x,t) \tag{16}$$

$$u_y(x,z,t) = 0, \tag{17}$$

$$u_z(x,z,t) = w(x,t) \tag{18}$$

where $u$ and $w$ denote the displacement components of the mid-surface in the $x$ and $z$ directions, respectively, and $\phi$ denotes the slope. Therefore, the Timoshenko strains are given by

$$\varepsilon_{xx} = \frac{\partial u_x}{\partial x} = \frac{\partial u}{\partial x} - z\frac{\partial \phi}{\partial x} \tag{19}$$

$$\gamma_{xz} = \frac{1}{2}\left(\frac{\partial w}{\partial x} - \phi\right) \tag{20}$$

$$\varepsilon_{yy} = \varepsilon_{zz} = \gamma_{xy} = \gamma_{yz} = 0. \tag{21}$$

Hamilton's principle is used in order to derive equation of motion, where

$$\delta \int_{t_1}^{t_2} [T - (U - V)]dt = 0 \tag{22}$$

Here $U$, $V$ and $T$ denote the strain energy, the potential energy of the external forces and the kinetic energy, respectively. The strain energy is defined as

$$\delta U = \int_V \sigma_{ij}\, \delta\epsilon_{ij} dV = \int_V (\sigma_{xx}\, \delta\epsilon_{xx} + \sigma_{xz}\delta\gamma_{xz})dV \tag{23}$$

Stress resultants are given as

$$N_{xx} = b\int_{-h/2}^{h/2} \sigma_{xx}(z)dz, \quad M_{xx} = b\int_{-h/2}^{h/2} z\sigma_{xx}(z)\, dz, \quad Q_{xz} = b\int_{-h/2}^{h/2} k_s\sigma_{xz}(z)dz \tag{24}$$

where $k_s$ is the shear correction factor.

In terms of the stress resultants, the variation of the strain energy is

$$\delta U = \int_0^L \left(N_{xx}\frac{\partial \delta u}{\partial x} - M_{xx}\frac{\partial \delta\phi}{\partial x} + Q_{xz}\frac{\partial \delta w}{\partial x} - Q_{xz}\delta\phi\right) dx \tag{25}$$

The variation of the kinetic energy is

$$\delta T = \int_0^L \rho(z)A\frac{\partial u_x}{\partial t}\delta\left(\frac{\partial u_x}{\partial t}\right) dx + \int_0^L \rho(z)A\frac{\partial u_z}{\partial t}\delta\left(\frac{\partial u_z}{\partial t}\right) dx$$

$$=\int_0^L (m_0 \frac{\partial u}{\partial t} - m_1 \frac{\partial \phi}{\partial t})\delta\left(\frac{\partial u}{\partial t}\right) dx + \int_0^L (m_2 \frac{\partial \phi}{\partial t} - m_1 \frac{\partial u}{\partial t})\delta\left(\frac{\partial \phi}{\partial t}\right) dx + \int_0^L (m_0 \frac{\partial w}{\partial t})\delta\left(\frac{\partial w}{\partial t}\right) dx \quad (26)$$

where the mass moments of inertia are defined as

$$\begin{Bmatrix} m_0 \\ m_1 \\ m_2 \end{Bmatrix} = b \int_{-h/2}^{h/2} \begin{Bmatrix} 1 \\ z \\ z^2 \end{Bmatrix} \rho(z) dz \quad (27)$$

The variation of the externally applied forces is defined as

$$\delta V = \iiint_V \left( f\delta u + q\delta w + P \frac{\partial w}{\partial x}\frac{\partial \delta w}{\partial x} \right) dV \quad (28)$$

where $f$, $q$ and $P$ denote the axial distributed forces, the transverse distributed forces and the axial concentrated force, respectively.

By substituting Eqs. (25), (26) and (28) into Eq. (22), performing integration by parts, and collecting coefficients of $\delta u$, $\delta\phi$ and $\delta w$ ,the equations of motion for a Timoshenko beam are obtained as

$$\delta u : \frac{\partial N_{xx}}{\partial x} - m_0 \frac{\partial^2 u}{\partial t^2} + m_1 \frac{\partial^2 \phi}{\partial t^2} + f = 0 \quad (29)$$

$$\delta \phi : Q_{xz} - \frac{\partial M_{xx}}{\partial x} - m_2 \frac{\partial^2 \phi}{\partial t^2} + m_1 \frac{\partial^2 u}{\partial t^2} = 0 \quad (30)$$

$$\delta w : \frac{\partial Q_{xz}}{\partial x} - m_0 \frac{\partial^2 w}{\partial t^2} + q - P \frac{\partial^2 w}{\partial x^2} = 0 \quad (31)$$

Furthermore, the mathematical process just derived provides the corresponding boundary conditions at $x = 0$ and $x = L$ as

$$\delta u \Longrightarrow \text{either} \quad N_{xx} = 0 \quad \text{or} \quad u = 0 \quad (32)$$

$$\delta \phi \Rightarrow \text{either} \quad M_{xx} = 0 \quad \text{or} \quad \phi = 0 \quad (33)$$

$$\delta w \Rightarrow \text{either} \quad Q_{xz} - P \frac{\partial w}{\partial x} = 0 \quad \text{or} \quad w = 0 \quad (34)$$

Substituting Eqs. (19) and (20) into Eqs. (14) and (15), and using (24), one the obtains stress resultants

$$N_{xx} = (ea_0)^2 \frac{\partial^2 N_{xx}}{\partial x^2} + (A_{xx} \frac{\partial u}{\partial x} - B_{xx} \frac{\partial \phi}{\partial x}), \quad (35)$$



ACCEPTED MANUSCRIPT

$$Q_{xz} = (ea_0)^2 \frac{\partial^2 Q_{xz}}{\partial x^2} + k_s A_{xz}(\frac{\partial w}{\partial x} - \phi), \tag{36}$$

$$M_{xx} = (ea_0)^2 \frac{\partial^2 M_{xx}}{\partial x^2} + \left(B_{xx}\frac{\partial u}{\partial x} - D_{xx}\frac{\partial \phi}{\partial x}\right). \tag{37}$$

Here the extensional coefficient $A_{xx}$, the extensional–bending coefficient $B_{xx}$, the bending coefficient $D_{xx}$ and the shear coefficient $A_{xz}$ are defined as

$$\begin{Bmatrix} A_{xx} \\ B_{xx} \\ D_{xx} \end{Bmatrix} = b\int_{-h/2}^{h/2} \begin{Bmatrix} 1 \\ z \\ z^2 \end{Bmatrix} E(z)dz \tag{38}$$

$$A_{xz} = b\int_{-h/2}^{h/2} k_s G(z)dz \tag{39}$$

In view of Eqs. (29)-(31), Eqs. (35)-(37) may be written in displacement form as

$$N_{xx} = (ea_0)^2(m_0\frac{\partial^3 u}{\partial x \partial t^2} - m_1\frac{\partial^3 \phi}{\partial x \partial t^2} - \frac{\partial f}{\partial x}) + (A_{xx}\frac{\partial u}{\partial x} - B_{xx}\frac{\partial \phi}{\partial x}), \tag{40}$$

$$Q_{xz} = (ea_0)^2(m_0\frac{\partial^3 w}{\partial x \partial t^2} - \frac{\partial q}{\partial x} + P\frac{\partial^3 w}{\partial x^3}) + k_s A_{xz}(\frac{\partial w}{\partial x} - \phi), \tag{41}$$

$$M_{xx} = (ea_0)^2(m_0\frac{\partial^2 w}{\partial t^2} - m_2\frac{\partial^3 \phi}{\partial x \partial t^2} + m_1\frac{\partial^3 u}{\partial x \partial t^2} + \frac{\partial f}{\partial x} + P\frac{\partial^2 w}{\partial x^2} - q) + \left(B_{xx}\frac{\partial u}{\partial x} - D_{xx}\frac{\partial \phi}{\partial x}\right). \tag{42}$$

By substituting Eqs. (40)-(42) into Eqs. (29)-(31) the governing equations of motion with respect to the displacements for a Timoshenko beam is derived as

$$\left(A_{xx}\frac{\partial^2 u}{\partial x^2} - B_{xx}\frac{\partial^2 \phi}{\partial x^2}\right) = (1 - (ea_0)^2\frac{\partial^2}{\partial x^2})(m_0\frac{\partial^2 u}{\partial t^2} - m_1\frac{\partial^2 \phi}{\partial t^2} - f), \tag{43}$$

$$\left(k_s A_{xz}\frac{\partial w}{\partial x} - k_s A_{xz}\phi - B_{xx}\frac{\partial^2 u}{\partial x^2} + D_{xx}\frac{\partial^2 \phi}{\partial x^2}\right)$$
$$= (ea_0)^2\left(m_1\frac{\partial^4 u}{\partial x^2 \partial t^2} - m_2\frac{\partial^4 \phi}{\partial x^2 \partial t^2}\right) + m_2\frac{\partial^2 \phi}{\partial t^2} - m_1\frac{\partial^2 u}{\partial t^2}. \tag{44}$$

$$k_s A_{xz}\left(\frac{\partial^2 w}{\partial x^2} - \frac{\partial \phi}{\partial x}\right) = (1 - (ea_0)^2\frac{\partial^2}{\partial x^2})(m_0\frac{\partial^2 w}{\partial t^2} - q + P\frac{\partial^2 w}{\partial x^2}), \tag{45}$$

Multiplying Eqs. (43)-(45) by $\delta u$, $\delta\phi$ and $\delta w$ respectively, and integrating over the beam length, the weak form is derived as



ACCEPTED MANUSCRIPT

$$\int_0^L \Big[\Big(A_{xx}\frac{\partial u}{\partial x}\frac{\partial \delta u}{\partial x} - B_{xx}\frac{\partial \phi}{\partial x}\frac{\partial \delta u}{\partial x}\Big) - \Big(1-(ea_0)^2\frac{\partial^2}{\partial x^2}\Big)\Big(m_0\frac{\partial^2 u}{\partial t^2}\delta u - m_1\frac{\partial^2 \phi}{\partial t^2}\delta u + f\delta u\Big) + (-k_sA_{xz}\frac{\partial w}{\partial x}\delta\phi + k_sA_{xz}\phi\delta\phi - B_{xx}\frac{\partial u}{\partial x}\frac{\partial \delta\phi}{\partial x} + D_{xx}\frac{\partial \phi}{\partial x}\frac{\partial \delta\phi}{\partial x}) + \Big(1-(ea_0)^2\frac{\partial^2}{\partial x^2}\Big)(-m_1\frac{\partial^2 u}{\partial t^2}\delta\phi + m_2\frac{\partial^2 \phi}{\partial t^2}\delta\phi) + k_sA_{xz}(-\phi\frac{\partial \delta w}{\partial x} + \frac{\partial w}{\partial x}\frac{\partial \delta w}{\partial x}) + \Big(1-(ea_0)^2\frac{\partial^2}{\partial x^2}\Big)(m_0\frac{\partial^2 w}{\partial t^2}\delta w + q\delta w + P\frac{\partial w}{\partial x}\frac{\partial \delta w}{\partial x})\Big]\,dx = 0. \quad (46)$$

In Eq. (46), by ignoring the time dependent terms, the weak form related to buckling is derived.

## 2.4 Finite element formulation

In Fig. 3 a five-node beam element, with four equally spaced nodes and one node at the middle is shown. This finite beam element has ten degrees-of freedom containing three axial, three rotational and four transverse displacements that are measured at the neutral axis. Accordingly, the nodal displacement vector is given by

$$\boldsymbol{q} = \{u_1\; u_2\; u_3\;\; w_1\; w_2\; w_3\; w_4\; \phi_1\; \phi_2\; \phi_3\}^T \quad (47)$$

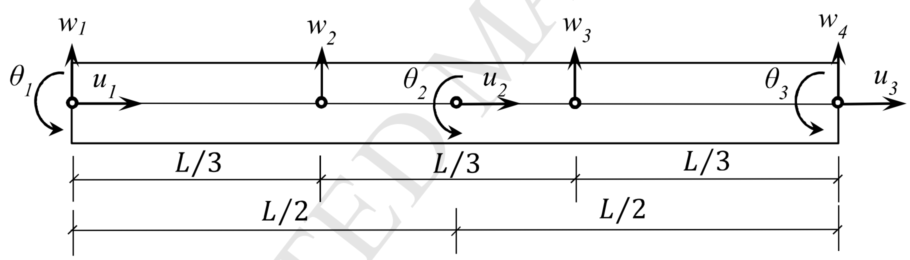


Fig. 3 Beam element with ten degrees of freedom.

The domain of the Timoshenko beam is discretized into a set of elements. The weak form is applied to each of the discrete elements of length $l_e$ with domain $\mho^e = (x_e, x_{e+1})$. Assuming that the solutions are given by $u(x,t) = \sum_{i=1}^{3}\varphi_i(x)e^{i\omega t}$, $w(x,t) = \sum_{i=1}^{4}\psi_i(x)e^{i\omega t}$, $\phi(x,t) = \sum_{i=1}^{3}\theta_i(x)e^{i\omega t}$ with no axial or transverse distributed forces, one obtains the general form of Eq. (46) for all nodes of a single element, as

$$\int_0^L \Big[\Big(A_{xx}\frac{\partial \varphi}{\partial x}\frac{\partial \delta\varphi}{\partial x} - B_{xx}\frac{\partial \theta}{\partial x}\frac{\partial \delta\varphi}{\partial x}\Big) + \Big(1-(ea_0)^2\frac{\partial^2}{\partial x^2}\Big)(m_0\omega^2\varphi\delta\varphi - m_1\omega^2\theta\delta\varphi) + (-k_sA_{xz}\frac{\partial \psi}{\partial x}\delta\theta + k_sA_{xz}\theta\delta\theta - B_{xx}\frac{\partial \varphi}{\partial x}\frac{\partial \delta\theta}{\partial x} + D_{xx}\frac{\partial \theta}{\partial x}\frac{\partial \delta\theta}{\partial x}) + \Big(1-(ea_0)^2\frac{\partial^2}{\partial x^2}\Big)(-m_1\omega^2\varphi\delta\theta + m_2\omega^2\theta\delta\theta) + k_sA_{xz}(-\theta\frac{\partial \delta\psi}{\partial x} + \frac{\partial \psi}{\partial x}\frac{\partial \delta\psi}{\partial x}) + \Big(1-(ea_0)^2\frac{\partial^2}{\partial x^2}\Big)(m_0\omega^2\psi\delta\psi + P\frac{\partial \psi}{\partial x}\frac{\partial \delta\psi}{\partial x})\Big]\,dx = 0. \quad (48)$$



ACCEPTED MANUSCRIPT

where $\varphi_i(x)$, $\psi_i(x)$ and $\theta_i(x)$ denote the shape functions. The axial displacement of a point which is not on the neutral axis is a linear function of both $u$ and $\phi$, and so the degrees of the polynomials for $\varphi_i(x)$ and $\theta_i(x)$ must have equal order. Furthermore, because the shear strain is a linear function of both the rotation $\phi$ and the slope of displacement, $\partial w/\partial x$, the degree of the polynomial for $\psi_i(x)$ has to be one order higher than $\varphi_i(x)$ and $\theta_i(x)$ in order to satisfy compatibility. One cubic polynomial for $\psi_i(x)$ and quadratic polynomials for $\varphi_i(x)$ and $\theta_i(x)$, which are derived by the Lagrange interpolation formula, are chosen for consistency [29,51] and given by

$$[\varphi_1, \theta_1] = (1-\zeta)(1-2\zeta), \quad [\varphi_2, \theta_2] = 4\zeta(1-\zeta), \quad [\varphi_3, \theta_3] = -\zeta(1-2\zeta),$$
$$\psi_1 = (1-\zeta)\left(1-\tfrac{3}{2}\zeta\right)(1-3\zeta), \quad \psi_2 = 9\zeta(1-\zeta)\left(1-\tfrac{3}{2}\zeta\right), \quad \psi_3 = \tfrac{-9}{2}\zeta(1-\zeta)(1-3\zeta),$$
$$\psi_4 = \zeta(1-3\zeta)\left(1-\tfrac{3}{2}\zeta\right). \tag{49}$$

Equation of motion for a beam is given as

$$\bar{\boldsymbol{M}}\ddot{\boldsymbol{U}} + \left(\bar{\boldsymbol{K}} - P\bar{\boldsymbol{K}}_p\right)\boldsymbol{U} = \boldsymbol{0} \tag{50}$$

where the $\bar{\boldsymbol{K}}$, $\bar{\boldsymbol{M}}$ and $\bar{\boldsymbol{K}}_p$ are the global stiffness, mass and geometric stiffness matrices, respectively. $\boldsymbol{U}$ is the displacement vector. For free vibration examinations, the following eigenvalue relation is deduced from Eq. 50

$$(\bar{\boldsymbol{K}} - \omega^2\bar{\boldsymbol{M}})\boldsymbol{U} = \boldsymbol{0} \tag{51}$$

Also, for buckling analysis, by neglecting time dependent terms in Eq. 50, the following is achieved

$$(\bar{\boldsymbol{K}} - P_{cr}\bar{\boldsymbol{K}}_p)\boldsymbol{U} = \boldsymbol{0} \tag{52}$$

The abovementioned global matrices, are deduced by employing the elemental matrices which are given below in a standard assembly procedure.

$$[\bar{\boldsymbol{K}}^{ij}] = \begin{bmatrix} k^{11} & 0 & k^{13} \\ 0 & k^{22} & k^{23} \\ k^{31} & k^{32} & k^{33} \end{bmatrix}, [\bar{\boldsymbol{K}}_P^{ij}] = \begin{bmatrix} 0 & 0 & 0 \\ 0 & k_p^{22} & 0 \\ 0 & 0 & 0 \end{bmatrix}, [\bar{\boldsymbol{M}}^{ij}] = \begin{bmatrix} m^{11} & 0 & m^{13} \\ 0 & m^{22} & 0 \\ m^{31} & 0 & m^{33} \end{bmatrix} \tag{53}$$

where

$$k^{11} = A_{xx}k_{aa1},\ k^{13} = -B_{xx}k_{aa1},\ k^{23} = -A_{xz}k_{bc1},\ k^{33} = k_sA_{xz}k_{aa} + D_{xx}k_{aa1},$$
$$k^{22} = k_sA_{xz}k_{bb1},\ m^{11} = m_0\omega^2k_{aa} + (ea_0)^2m_0\omega^2k_{aa1},\ m^{13} = -m_1\omega^2k_{aa}(ea_0)^2m_1\omega^2k_{aa1},$$
$$m^{33} = m_2\omega^2k_{aa} + (ea_0)^2m_2\omega^2k_{aa1},\ m^{22} = m_0\omega^2k_{bb} + (ea_0)^2m_0\omega^2k_{bb1},$$
$$k_p^{22} = k_{bb1} + (ea_0)^2k_{bb2}. \tag{54}$$

These matrices are explicitly defined in Appendix A.

# 3. Numerical results

## 3.1 Validation

This section is composed of two parts. Section 3.1.1 provides validation for vibration and buckling of a functionally graded Timoshenko beam and Section 3.1.2 presents a validation study for the nonlocal elasticity formulation of the present model.

### 3.1.1 Free vibration and buckling of a functionally graded Timoshenko beam

A convergence study is performed first for the proposed finite element. Unless otherwise stated, a functionally graded beam composed of aluminum ($Al$) as the metal and alumina ($Al_2O_3$) as the ceramic is considered, in which $E_m = 70\text{GPa}$, $\rho_m = 2702\ \text{kg/m}^3$, $\upsilon_m = 0.3$, $E_c = 380\text{GPa}$, $\rho_c = 3960\ \text{kg/m}^3$ and $\upsilon_c = 0.3$ [52]. For the buckling studies, in order to have a comparison with Li & Batra [53], $\upsilon_m = \upsilon_c = 0.23$ is employed. It should be mentioned that all of the references used for comparison in this section have assumed the coincidence of the cross-sectional geometric and elastic centres. Tables 1 and 2 give the nondimensional natural frequencies and critical buckling loads respectively, for functionally graded beams with various boundary conditions for $L/h = 5$ and $k = 1$. The rapid convergence of the proposed element can be seen in Tables 1 and 2. Furthermore, the results of the present element are in a good agreement with the analytical and numerical values reported by [52], [53] and [30].

ACCEPTED MANUSCRIPT

Table1. Nondimensional frequency $\widehat{\omega} = \omega\, L^2/h\,\sqrt{\rho_m/E_m}$.

| Mode | Pinned-pinned | | | | | | | | | |
|---|---|---|---|---|---|---|---|---|---|---|
| | Number of elements | | | | | | | | | |
| | 2 | 6 | 10 | 14 | 18 | 22 | 25 | 26 | Simsek [52] | Kahya & Turan [30] |
| 1 | 3.9850 | 3.9710 | 3.9708 | 3.9708 | 3.9708 | 3.9708 | 3.9708 | 3.9708 | 3.9902 | 3.9708 |
| 2 | 12.1786 | 12.0971 | 12.0963 | 12.0962 | 12.0962 | 12.0962 | 12.0962 | 12.0962 | - | - |
| 3 | 15.5291 | 14.4210 | 14.4140 | 14.4132 | 14.413 | 14.4129 | 14.4129 | 14.4129 | - | - |
| | Fixed-fixed | | | | | | | | | |
| | Number of elements | | | | | | | | | |
| | 2 | 6 | 10 | 14 | 18 | 22 | 25 | 26 | Simsek [52] | Kahya & Turan [30] |
| 1 | 7.9927 | 7.9012 | 7.8999 | 7.8998 | 7.8997 | 7.8997 | 7.8997 | 7.8997 | 7.9252 | 7.8992 |
| 2 | 21.0862 | 18.3211 | 18.3044 | 18.3025 | 18.3021 | 18.3020 | 18.3019 | 18.3019 | - | - |
| 3 | 25.4111 | 25.2976 | 25.2963 | 25.2962 | 25.2962 | 25.2962 | 25.2962 | 25.2962 | - | - |
| | Fixed-free | | | | | | | | | |
| | Number of elements | | | | | | | | | |
| | 2 | 6 | 10 | 14 | 18 | 22 | 25 | 26 | Simsek [52] | Kahya & Turan [30] |
| 1 | 1.4634 | 1.4628 | 1.4627 | 1.4627 | 1.4627 | 1.4627 | 1.4627 | 1.4627 | 1.4630 | 1.4627 |
| 2 | 8.0267 | 7.9731 | 7.9718 | 7.9717 | 7.9717 | 7.9717 | 7.9717 | 7.9717 | - | - |
| 3 | 12.711 | 12.7061 | 12.7060 | 12.7060 | 12.7060 | 12.7060 | 12.7060 | 12.7060 | - | - |

ACCEPTED MANUSCRIPT

Table 2. Nondimensional buckling load $\hat{P} = P \times 12L^2/E_m h^3$.

| Pinned-pinned | | | | | | | | | | | | |
|---|---|---|---|---|---|---|---|---|---|---|---|---|
| | Number of elements | | | | | | | | | | | |
| Mode | 2 | 6 | 10 | 14 | 18 | 22 | 30 | 38 | 42 | 43 | Li & Batra [53] | Kahya & Turan [30] |
| 1 | 24.8586 | 24.6894 | 24.6874 | 24.6871 | 24.6871 | 24.6871 | 24.6871 | 24.6871 | 24.6871 | 24.6871 | 24.687 | 24.6871 |
| 2 | 92.9300 | 80.5933 | 80.5103 | 80.5008 | 80.4987 | 80.4981 | 80.4977 | 80.4976 | 80.4975 | 80.4975 | - | - |
| 3 | 168.5654 | 139.0647 | 138.5501 | 138.4888 | 138.4747 | 138.4702 | 138.4676 | 138.4670 | 138.4668 | 138.4668 | - | - |
| Fixed-fixed | | | | | | | | | | | | |
| | Number of elements | | | | | | | | | | | |
| Mode | 2 | 6 | 10 | 14 | 18 | 22 | 30 | 38 | 42 | 43 | Li & Batra [53] | Kahya & Turan [30] |
| 1 | 81.2963 | 80.5934 | 80.5104 | 80.5009 | 80.4987 | 80.4981 | 80.4977 | 80.4976 | 80.4975 | 80.4975 | 80.498 | 80.4983 |
| 2 | 156.8757 | 126.4330 | 126.0977 | 126.0571 | 126.0478 | 126.0448 | 126.0430 | 126.0426 | 126.0425 | 126.0425 | - | - |
| 3 | 295.4309 | 186.8627 | 185.3840 | 185.1968 | 185.1532 | 185.1390 | 185.1308 | 185.1287 | 185.1282 | 185.1282 | - | - |
| Fixed-free | | | | | | | | | | | | |
| | Number of elements | | | | | | | | | | | |
| Mode | 2 | 6 | 10 | 14 | 18 | 22 | 30 | 38 | 42 | 43 | Li & Batra [53] | Kahya & Turan [30] |
| 1 | 6.5459 | 6.5426 | 6.5426 | 6.5426 | 6.5426 | 6.5426 | 6.5426 | 6.5426 | 6.5426 | 6.5426 | 6.6002 | 6.5426 |
| 2 | 52.1717 | 50.7734 | 50.7544 | 50.7522 | 50.7517 | 50.7516 | 50.7515 | 50.7515 | 50.7515 | 50.7515 | - | - |
| 3 | 127.2740 | 110.7389 | 110.5024 | 110.4749 | 110.4686 | 110.4666 | 110.4655 | 110.4652 | 110.4652 | 110.4652 | - | - |

Another comparison is made for the nondimensional fundamental frequencies and critical buckling loads of FGBs with various boundary conditions for $L/h = 5$ in Tables 3 and 4, respectively. The results of the present model are compared to the results for different higher-order beam theories such as parabolic shear deformation theory (PSDBT) [52], higher-order shear deformation theory (HSDBT) [54], Reddy-Bickford beam theory (RBT) [55], a quasi-3D theory [56] and first order shear deformation theory (FSDBT) [15]. Note that the results obtained by Simsek [52] and Nguyen [54] are based on analytical solutions, while the rest of the investigations are performed by the finite element method (Vo et al. [55], Vo et al. [56] and Kahya & Turan [30]). According to these tables, the proposed finite element model is in a good agreement with the two analytical and three finite element references. These two tables complete the validation study for vibration and buckling response of a local functionally graded beam.

Table 3. Comparison of the nondimensional fundamental frequencies $\widehat{\omega} = \omega\, L^2/h\sqrt{\rho_m/E_m}$ of functionally graded beams with various boundary conditions and power-law exponents ($L/h = 5$).

| Pin-pin | | | | | | |
|---|---|---|---|---|---|---|
| $k$ | PSDBT Simsek [52] | HSDBT Nguyen et al. [54] | RBT Vo et al. [55] | Quasi-3D Vo et al. [56] | FSDBT Kahya &Turan [30] | FSDBT Present |
| 0 | 5.15274 | 5.1528 | 5.1528 | 5.1618 | 5.22193 | 5.1525 |
| 0.5 | 4.41108 | 4.4102 | 4.4019 | 4.4240 | 4.46926 | 4.2312 |
| 1 | 3.99042 | 3.9904 | 3.9716 | 4.0079 | 4.04967 | 3.9708 |
| 2 | 3.62643 | 3.6264 | 3.5979 | 3.6442 | 3.69360 | 3.7051 |
| 5 | 3.40120 | 3.4009 | 3.3743 | 3.4133 | 3.48818 | 3.3605 |
| 10 | 3.28160 | 3.2815 | 3.2653 | 3.2903 | 3.36434 | 3.1307 |
| ∞ | 2.67732 | - | - | - | 2.71328 | 2.6771 |
| Fixed-fixed | | | | | | |
| $k$ | PSDBT Simsek [52] | HSDBT Nguyen et al. [54] | RBT Vo et al. [55] | Quasi-3D Vo et al. [56] | FSDBT Kahya &Turan [30] | FSDBT Present |
| 0 | 10.0705 | 10.0726 | 10.0678 | 10.1851 | 10.08647 | 9.9975 |
| 0.5 | 8.7467 | 8.7463 | 8.7457 | 8.8641 | 8.75479 | 8.4251 |
| 1 | 7.9503 | 7.9518 | 7.9522 | 8.0770 | 7.98414 | 7.8998 |
| 2 | 7.1767 | 7.1776 | 7.1801 | 7.3039 | 7.27155 | 7.3228 |
| 5 | 6.49349 | 6.4929 | 6.4961 | 6.5960 | 6.71481 | 6.5579 |
| 10 | 6.16515 | 6.1658 | 6.1662 | 6.2475 | 6.37413 | 6.0695 |
| ∞ | 5.23254 | - | - | - | 5.24085 | 5.1946 |
| Fixed-free | | | | | | |
| $k$ | PSDBT Simsek [52] | HSDBT Nguyen et al. [54] | RBT Vo et al. [55] | Quasi-3D Vo et al. [56] | FSDBT Kahya &Turan [30] | FSDBT Present |
| 0 | 1.89523 | 1.8957 | 1.8952 | 1.9055 | 1.90772 | 1.8944 |
| 0.5 | 1.61817 | 1.6182 | 1.6180 | 1.6313 | 1.62865 | 1.5547 |
| 1 | 1.46328 | 1.4636 | 1.4633 | 1.4804 | 1.47394 | 1.4627 |
| 2 | 1.33254 | 1.3328 | 1.3326 | 1.3524 | 1.34469 | 1.3674 |
| 5 | 1.25916 | 1.2594 | 1.2592 | 1.2763 | 1.27515 | 1.2401 |
| 10 | 1.21834 | 1.2187 | 1.2184 | 1.2308 | 1.26363 | 1.1540 |
| ∞ | 0.98474 | - | - | - | 0.99124 | 0.9843 |

Table 4. Comparison of the nondimensional critical buckling loads $\hat{P} = P \times 12L^2/E_m h^3$ of functionally graded beams with various boundary conditions and power-law exponents ($L/h = 5$).

| Pin-pin | | | | | |
|---|---|---|---|---|---|
| $k$ | HSDBT Nguyen et al. [54] | RBT Vo et al. [55] | Quasi-3D Vo et al. [56] | FSDBT Kahya &Turan [30] | FSDBT Present |
| 0 | 48.8406 | 48.8401 | 49.5901 | 48.5907 | 48.8352 |
| 0.5 | 32.0013 | 32.0094 | 32.5867 | 31.8238 | 29.6502 |
| 1 | 24.6894 | 24.6911 | 25.2116 | 24.5815 | 24.6871 |
| 2 | 19.1577 | 19.1605 | 19.6124 | 19.1617 | 20.1763 |
| 5 | 15.7355 | 15.7400 | 16.0842 | 15.9417 | 15.4179 |
| 10 | 14.1448 | 14.1468 | 14.4116 | 14.3445 | 12.8853 |
| ∞ | - | - | - | 8.95100 | 8.9959 |
| Fixed-fixed | | | | | |
| $k$ | HSDBT Nguyen et al. [54] | RBT Vo et al. [55] | Quasi-3D Vo et al. [56] | FSDBT Kahya &Turan [30] | FSDBT Present |
| 0 | 154.5610 | 154.5500 | 160.1070 | 151.9430 | 154.3511 |
| 0.5 | 103.7167 | 103.7490 | 107.6550 | 101.7439 | 97.0980 |
| 1 | 80.5940 | 80.6087 | 83.6958 | 79.3903 | 80.4975 |
| 2 | 61.7666 | 61.7925 | 64.1227 | 61.7449 | 65.0569 |
| 5 | 47.7174 | 47.7562 | 49.3856 | 49.5828 | 48.8738 |
| 10 | 41.7885 | 41.8042 | 43.1579 | 43.5014 | 40.5455 |
| ∞ | - | - | - | 27.9896 | 28.4331 |
| Fixed-free | | | | | |
| $k$ | HSDBT Nguyen et al. [54] | RBT Vo et al. [55] | Quasi-3D Vo et al. [56] | FSDBT Kahya &Turan [30] | FSDBT Present |
| 0 | 13.0771 | 13.0771 | 13.0993 | 13.0594 | 13.0769 |
| 0.5 | 8.5000 | 8.5020 | 8.5469 | 8.4899 | 7.8469 |
| 1 | 6.5427 | 6.5428 | 6.6067 | 6.5352 | 6.5426 |
| 2 | 5.0977 | 5.0979 | 5.1680 | 5.0981 | 5.3667 |
| 5 | 4.2772 | 4.2776 | 4.3290 | 4.2926 | 4.1245 |
| 10 | 3.8820 | 3.8821 | 3.9121 | 3.8970 | 3.4556 |
| ∞ | - | - | - | 2.40570 | 2.4089 |

## 3.1.2 Free vibration and buckling of a homogeneous nanobeam using nonlocal elasticity

In this section, the validation procedure continues by comparing the nondimensional fundamental natural frequencies and critical buckling loads of homogenous nonlocal beams with four nonlocal beam theories including the Euler-Bernoulli (EBT), the first order shear deformation theory (FSDBT), the Reddy beam theory (RBT) and the Levinson beam theory (LBT). The results from the proposed finite element model are compared to the analytical solutions of Reddy [57] in Tables 5 and 6 with different nonlocal parameters. The material properties are identical to those given by Reddy [57], that is $L = 10\text{m}$, $E = 30 \times 10^6\text{Pa}$, $\nu =$

0.3, $\rho = 1\,\text{kg/m}^3$. Although, the proposed beam element is based on a simpler beam theory compared to RBT and LBT, there are very accurate estimates for the fundamental natural frequencies and the critical buckling loads.

Table 5. Non-dimensional fundamental natural frequencies ($\widehat{\omega} = \frac{\omega L}{h}\sqrt{\rho/E}$) of simply supported beams.

| $L/h$ | $(ea_0)^2[m^2]$ | Theory | | | | |
|---|---|---|---|---|---|---|
| | | EBT Reddy[57] | FSDBT[a] Reddy[57] | RBT Reddy[57] | LBT Reddy[57] | FSDBT[a] Present |
| 100 | 0 | 9.8696 | 9.8683 | 9.8683 | 9.8685 | 9.8679 |
| | 0.5 | 9.6347 | 9.6335 | 9.6335 | 9.6337 | 9.6331 |
| | 1.0 | 9.4159 | 9.4147 | 9.4147 | 9.4149 | 9.4143 |
| | 1.5 | 9.2113 | 9.2101 | 9.2101 | 9.2103 | 9.2097 |
| | 2.0 | 9.0195 | 9.0183 | 9.0183 | 9.0185 | 9.0180 |
| | 2.5 | 8.8392 | 8.8380 | 8.8380 | 8.8382 | 8.8377 |
| | 3.0 | 8.6693 | 8.6682 | 8.6682 | 8.6683 | 8.6678 |
| | 3.5 | 8.5088 | 8.5077 | 8.5077 | 8.5079 | 8.5073 |
| | 4.0 | 8.3569 | 8.3558 | 8.3558 | 8.3560 | 8.3555 |
| | 4.5 | 8.2129 | 8.2118 | 8.2118 | 8.2120 | 8.2115 |
| | 5.0 | 8.0761 | 8.0750 | 8.0750 | 8.0752 | 8.0747 |

[a] shear correction factor $K_s = 5/6$.

Table 6. Non-dimensional critical buckling load ($\hat{P} = PL^2/EI$) of simply supported beams.

| $L/h$ | $(ea_0)^2[m^2]$ | Theory | | | | |
|---|---|---|---|---|---|---|
| | | EBT Reddy[57] | FSDBT[a] Reddy[57] | RBT Reddy[57] | LBT Reddy[57] | FSDBT[a] Present |
| 100 | 0 | 9.8696 | 9.8671 | 9.8671 | 9.8675 | 9.8670 |
| | 0.5 | 9.4055 | 9.4031 | 9.4031 | 9.4035 | 9.3989 |
| | 1.0 | 8.9830 | 8.9807 | 8.9807 | 8.9811 | 8.9663 |
| | 1.5 | 8.5969 | 8.5947 | 8.5947 | 8.5950 | 8.5661 |
| | 2.0 | 8.2426 | 8.2405 | 8.2405 | 8.2408 | 8.1956 |
| | 2.5 | 7.9163 | 7.9143 | 7.9143 | 7.9146 | 7.8520 |
| | 3.0 | 7.6149 | 7.6130 | 7.6130 | 7.6133 | 7.5331 |
| | 3.5 | 7.3356 | 7.3337 | 7.3337 | 7.3340 | 7.2366 |
| | 4.0 | 7.0761 | 7.0743 | 7.0743 | 7.0746 | 6.9603 |
| | 4.5 | 6.8343 | 6.8325 | 6.8325 | 6.8328 | 6.7027 |
| | 5.0 | 6.6085 | 6.6068 | 6.6068 | 6.6070 | 6.4620 |

[a] shear correction factor $K_s = 5/6$.

For further validation, Table 7 compares the fundamental frequencies of the proposed nonlocal beam element with three numerical investigations including those of Pradhan and Phadikar [58] based on differential quadrature method (DQM) and Phadikar and Pradhan [22], and Aria and Biglari [59] using the finite element method. Here, the fundamental natural frequencies are tabulated for various boundary conditions and three modes of vibration. It can be seen that there is a good agreement between the results of the proposed finite element model and the literature. Another validation for the buckling of nonlocal beams is performed in Table 8, where the critical



ACCEPTED MANUSCRIPT

buckling loads for different boundary conditions are given and compared with the present study. This table also shows satisfactory results for the proposed element and hence the validation procedure of this study is achieved.

Table 7. Non-dimensional fundamental natural frequencies ($\hat{\omega} = \frac{\omega L}{h}\sqrt{\rho/E}$) for different boundary conditions ($L = 1m, E = 1Pa, I = 1m^4, A = 1m^2$).

| $(ea_0)^2[m^2]$ | Boundary condition | Mode No. | DQM Pradhan& Phadikar [58] | FEM Phadikar& Pradhan [22] | FEM Aria& Biglari [59] | FEM[a] (present) |
|---|---|---|---|---|---|---|
| 0 | Pinned-pinned | 1 | 9.8696 | 9.8697 | 9.8696 | 9.8698 |
| | | 2 | 39.4784 | 39.4848 | 39.4784 | 39.4790 |
| | | 3 | 88.8249 | 88.8984 | 88.8264 | 88.8346 |
| | Fixed-pinned | 1 | 15.4182 | 15.4186 | - | 15.4180 |
| | | 2 | 49.9648 | 49.9779 | - | 49.9659 |
| | | 3 | 104.2471 | 104.3637 | - | 104.2608 |
| | Fixed-fixed | 1 | 22.3733 | 22.3745 | 22.3722 | 22.3732 |
| | | 2 | 61.6728 | 61.6973 | 61.6728 | 61.6750 |
| | | 3 | 120.9021 | 121.0840 | 120.9033 | 120.9238 |
| 1 | Pinned-pinned | 1 | 2.9936 | 2.9936 | 2.9936 | 2.9935 |
| | | 2 | 6.2051 | 6.2061 | 6.2051 | 6.2051 |
| | | 3 | 9.3720 | 9.3796 | 9.3720 | 9.3730 |
| | Fixed-pinned | 1 | 4.3182 | 4.3184 | - | 4.3182 |
| | | 2 | 7.6211 | 7.6238 | - | 7.6214 |
| | | 3 | 10.8302 | 10.8448 | - | 10.8317 |
| | Fixed-fixed | 1 | 6.0566 | 6.0574 | 6.0565 | 6.0566 |
| | | 2 | 8.8954 | 8.9011 | 8.8956 | 8.8960 |
| | | 3 | 12.4525 | 12.4822 | 12.4530 | 12.4567 |

[a] shear correction factor $K_s = 5/6$.

Table 8. Non-dimensional critical buckling load ($\hat{P} = PL^2/EI$) for different boundary conditions ($L = 1m, E = 1Pa, I = 1m^4, A = 1m^2$).

| $(ea_0)^2[m^2]$ | Boundary condition | DQM Pradhan& Phadikar [58] | FEM Phadikar& Pradhan [22] | FEM[a] (present) |
|---|---|---|---|---|
| 0 | Pinned-pinned | 9.8696 | 9.8747 | 9.8696 |
| | Fixed-free | 2.4749 | 2.4675 | 2.4674 |
| | Fixed-pinned | 20.1907 | 20.2322 | 20.1908 |
| | Fixed-fixed | 39.4784 | 39.7753 | 39.4797 |
| 1 | Pinned-pinned | 0.9080 | 0.9080 | 0.9074 |
| | Fixed-free | 0.7115 | 0.7116 | 0.7113 |
| | Fixed- | 0.9528 | 0.9259 | 0.9521 |



ACCEPTED MANUSCRIPT

| | | | | |
|---|---|---|---|---|
| | pinned | | | |
| | Fixed-fixed | 0.9753 | 0.9755 | 0.9746 |

[a] shear correction factor $K_s = 5/6$.

## 3.2 **Results and discussion**

To examine the importance of utilizing nonlocal FGMs on the free vibration and buckling responses of Timoshenko beams, here an FG beam is considered with the same material properties as Section 3.1.1. In this section the position of the neutral axis is calculated in order to determine elastic center. The natural frequencies and critical buckling loads are analyzed for different through thickness material distributions of FG beams and various nonlocal parameters.

The nondimensional fundamental natural frequencies of FG nanobeams for various nonlocal parameters and pinned-pinned, fixed-free, fixed-pinned and fixed-fixed boundary conditions are given in Tables 9-12. The results are tabulated for pure aluminum $Al$ ($k = 0$), pure alumina $Al_2O_3$ ($k \to \infty$) and for FGMs, which are combinations of these two materials. It can be realized from Tables 9-12 that increasing the power law exponent and also the nonlocal parameter causes a reduction in the frequency for all types of boundary conditions. Specifically, for a constant power law exponent (i.e. $k = 0$) with $L/h = 20$ by changing nonlocal parameter from $0\ \mathrm{m}^2$ to $5\ \mathrm{m}^2$, the nondimensional natural frequency decreases by 5.6%, 2.7%, 6.5% and 6.8% for pinned-pinned, fixed-free, fixed-pinned and fixed-fixed boundary conditions, respectively. It is observed that, for the fixed-fixed BC, the variation of the nonlocal parameter has the most influence on the variation of natural frequency, while this influence is the lowest for the fixed-free boundary condition. Also, for all of the nonlocal parameters with $L/h = 20{,}100$, by changing power law exponent from 0 to $\infty$, the nondimensional natural frequency decreases by 48% for all types of BCs (pinned-pinned, fixed-free, fixed-pinned and fixed-fixed). This highlights an important fact regarding the relation between the nonlocal parameter and the boundary conditions; the variation of the natural frequencies of an FGM nanobeam with nonlocal parameter depends on the boundary conditions while its variation with the power law exponent is the same for different types of BCs.

Table 9. Nondimensional fundamental natural frequencies of FGBs with varying nonlocal parameter for a pinned-pinned nanobeam.

| $(ea_0)^2[m^2]$ | $k = 0$ | $k = 0.1$ | $k = 0.2$ | $k = 0.5$ | $k = 1$ | $k = 2$ | $k = 5$ | $k = 10$ | $k \to \infty$ |
|---|---|---|---|---|---|---|---|---|---|
| $L/h = 20$ | | | | | | | | | |
| 0 | 5.4603 | 5.1841 | 5.0233 | 4.7506 | 4.5336 | 11.7405 | 12.6243 | 9.2014 | 2.8371 |
| 1 | 5.3941 | 5.1213 | 4.9624 | 4.693 | 4.4787 | 11.5983 | 12.4715 | 9.0900 | 2.8028 |
| 2 | 5.3303 | 5.0607 | 4.9037 | 4.6375 | 4.4257 | 11.4613 | 12.3241 | 8.9825 | 2.7696 |
| 3 | 5.2688 | 5.0023 | 4.8471 | 4.584 | 4.3746 | 11.3289 | 12.1817 | 8.8788 | 2.7376 |
| 4 | 5.2093 | 4.9458 | 4.7923 | 4.5322 | 4.3252 | 11.2011 | 12.0443 | 8.7785 | 2.7067 |
| 5 | 5.1517 | 4.8912 | 4.7394 | 4.4822 | 4.2775 | 11.0775 | 11.9113 | 8.6816 | 2.6768 |
| $L/h = 100$ | | | | | | | | | |
| 0 | 5.4824 | 5.2039 | 5.0421 | 4.7685 | 4.5515 | 56.7696 | 61.7651 | 44.4031 | 2.8486 |
| 1 | 5.4797 | 5.2014 | 5.0396 | 4.7661 | 4.5493 | 56.7416 | 61.7346 | 44.3812 | 2.8472 |
| 2 | 5.4770 | 5.1988 | 5.0372 | 4.7638 | 4.5471 | 56.7137 | 61.7042 | 44.3593 | 2.8458 |

| | | | | | | | | | |
|---|---|---|---|---|---|---|---|---|---|
| 3 | 5.4743 | 5.1962 | 5.0347 | 4.7614 | 4.5448 | 56.6858 | 61.6738 | 44.3375 | 2.8444 |
| 4 | 5.4716 | 5.1937 | 5.0322 | 4.7591 | 4.5426 | 56.6579 | 61.6435 | 44.3157 | 2.843 |
| 5 | 5.4689 | 5.1911 | 5.0297 | 4.7568 | 4.5404 | 56.6301 | 61.6132 | 44.2939 | 2.8416 |

Table 10. Nondimensional fundamental natural frequencies of FGBs with varying nonlocal parameter for a fixed-free nanobeam.

| $(ea_0)^2[m^2]$ | $k=0$ | $k=0.1$ | $k=0.2$ | $k=0.5$ | $k=1$ | $k=2$ | $k=5$ | $k=10$ | $k\to\infty$ |
|---|---|---|---|---|---|---|---|---|---|
| $L/h=20$ | | | | | | | | | |
| 0 | 1.9495 | 1.8507 | 1.7932 | 1.696 | 1.6188 | 6.4382 | 6.8303 | 5.0543 | 1.013 |
| 1 | 1.9383 | 1.8401 | 1.7829 | 1.6862 | 1.6095 | 6.4163 | 6.8075 | 5.0371 | 1.0071 |
| 2 | 1.9273 | 1.8296 | 1.7728 | 1.6766 | 1.6003 | 6.3946 | 6.7849 | 5.0201 | 1.0014 |
| 3 | 1.9164 | 1.8193 | 1.7628 | 1.6672 | 1.5913 | 6.3732 | 6.7625 | 5.0032 | 0.9958 |
| 4 | 1.9057 | 1.8091 | 1.7529 | 1.6579 | 1.5824 | 6.3519 | 6.7404 | 4.9865 | 0.9902 |
| 5 | 1.8952 | 1.7991 | 1.7433 | 1.6487 | 1.5736 | 6.3308 | 6.7184 | 4.9699 | 0.9847 |
| $L/h=100$ | | | | | | | | | |
| 0 | 1.9533 | 1.854 | 1.7964 | 1.6989 | 1.6216 | 29.0404 | 31.4625 | 22.7287 | 1.0149 |
| 1 | 1.9528 | 1.8536 | 1.796 | 1.6985 | 1.6212 | 29.0367 | 31.4586 | 22.7259 | 1.0147 |
| 2 | 1.9524 | 1.8532 | 1.7956 | 1.6981 | 1.6209 | 29.0331 | 31.4546 | 22.723 | 1.0144 |
| 3 | 1.9519 | 1.8527 | 1.7951 | 1.6977 | 1.6205 | 29.0294 | 31.4507 | 22.7201 | 1.0142 |
| 4 | 1.9514 | 1.8523 | 1.7947 | 1.6973 | 1.6201 | 29.0257 | 31.4467 | 22.7173 | 1.014 |
| 5 | 1.951 | 1.8519 | 1.7943 | 1.6969 | 1.6197 | 29.0221 | 31.4428 | 22.7144 | 1.0137 |

Table 11. Nondimensional fundamental natural frequencies of FGBs with varying nonlocal parameter for a fixed-pinned nanobeam.

| $(ea_0)^2[m^2]$ | $k=0$ | $k=0.1$ | $k=0.2$ | $k=0.5$ | $k=1$ | $k=2$ | $k=5$ | $k=10$ | $k\to\infty$ |
|---|---|---|---|---|---|---|---|---|---|
| $L/h=20$ | | | | | | | | | |
| 0 | 8.4813 | 8.0591 | 7.8176 | 7.4176 | 7.1106 | 13.1859 | 13.8712 | 10.3556 | 4.4068 |
| 1 | 8.3621 | 7.9458 | 7.7077 | 7.3134 | 7.0108 | 13.0095 | 13.6888 | 10.2168 | 4.3449 |
| 2 | 8.2476 | 7.837 | 7.6023 | 7.2133 | 6.915 | 12.8397 | 13.5132 | 10.0833 | 4.2854 |
| 3 | 8.1377 | 7.7325 | 7.5009 | 7.1172 | 6.8229 | 12.6762 | 13.3439 | 9.9546 | 4.2283 |
| 4 | 8.0319 | 7.632 | 7.4034 | 7.0247 | 6.7344 | 12.5186 | 13.1807 | 9.8306 | 4.1733 |
| 5 | 7.9301 | 7.5352 | 7.3095 | 6.9357 | 6.6491 | 12.3665 | 13.0231 | 9.7109 | 4.1204 |
| $L/h=100$ | | | | | | | | | |
| 0 | 8.5626 | 8.1314 | 7.8859 | 7.4812 | 7.1728 | 58.1436 | 62.9689 | 45.5078 | 4.4491 |
| 1 | 8.5576 | 8.1268 | 7.8814 | 7.4769 | 7.1687 | 58.1143 | 62.9372 | 45.4849 | 4.4465 |
| 2 | 8.5527 | 8.1221 | 7.8769 | 7.4726 | 7.1646 | 58.085 | 62.9057 | 45.4619 | 4.444 |
| 3 | 8.5478 | 8.1174 | 7.8724 | 7.4683 | 7.1605 | 58.0557 | 62.8741 | 45.439 | 4.4414 |
| 4 | 8.5429 | 8.1128 | 7.8679 | 7.464 | 7.1564 | 58.0265 | 62.8426 | 45.4161 | 4.4389 |
| 5 | 8.538 | 8.1081 | 7.8633 | 7.4598 | 7.1523 | 57.9974 | 62.8112 | 45.3933 | 4.4363 |

Table 12. Nondimensional fundamental natural frequencies of FGBs with varying nonlocal parameter for a fixed-fixed nanobeam.

| $(ea_0)^2[m^2]$ | $k=0$ | $k=0.1$ | $k=0.2$ | $k=0.5$ | $k=1$ | $k=2$ | $k=5$ | $k=10$ | $k\to\infty$ |
|---|---|---|---|---|---|---|---|---|---|
| $L/h=20$ | | | | | | | | | |
| 0 | 12.2201 | 11.6121 | 11.2563 | 10.6496 | 10.1633 | 14.7594 | 15.2026 | 11.6303 | 6.3495 |
| 1 | 12.0372 | 11.4382 | 11.0877 | 10.49 | 10.0109 | 14.5456 | 14.9888 | 11.4615 | 6.2545 |
| 2 | 11.862 | 11.2717 | 10.9262 | 10.3371 | 9.865 | 14.3403 | 14.7832 | 11.2994 | 6.1635 |

| | | | | | | | | | |
|---|---|---|---|---|---|---|---|---|---|
| 3 | 11.694 | 11.112 | 10.7713 | 10.1906 | 9.7251 | 14.1427 | 14.5854 | 11.1434 | 6.0762 |
| 4 | 11.5328 | 10.9586 | 10.6227 | 10.0499 | 9.5908 | 13.9526 | 14.3947 | 10.9933 | 5.9924 |
| 5 | 11.3778 | 10.8113 | 10.4798 | 9.9147 | 9.4618 | 13.7694 | 14.2109 | 10.8487 | 5.9119 |
| $L/h = 100$ | | | | | | | | | |
| 0 | 12.4215 | 11.791 | 11.4246 | 10.8047 | 10.3132 | 59.5421 | 64.1903 | 46.6357 | 6.4541 |
| 1 | 12.4138 | 11.7837 | 11.4175 | 10.7981 | 10.3068 | 59.5114 | 64.1575 | 46.6116 | 6.4502 |
| 2 | 12.4062 | 11.7765 | 11.4105 | 10.7914 | 10.3005 | 59.4808 | 64.1247 | 46.5876 | 6.4462 |
| 3 | 12.3986 | 11.7693 | 11.4035 | 10.7848 | 10.2942 | 59.4502 | 64.092 | 46.5636 | 6.4423 |
| 4 | 12.391 | 11.7621 | 11.3966 | 10.7782 | 10.2879 | 59.4196 | 64.0593 | 46.5396 | 6.4383 |
| 5 | 12.3834 | 11.7549 | 11.3896 | 10.7716 | 10.2816 | 59.3891 | 64.0267 | 46.5157 | 6.4344 |

The nondimensional critical buckling loads of FG nanobeams for different nonlocal parameters and pinned-pinned, fixed-free, fixed-pinned and fixed-fixed boundary conditions are reported in Tables 13-16. Once again, the material properties are given in Section 3.1.1. The results are calculated for pure aluminum $Al$ ($k = 0$), pure alumina $Al_2O_3$ ($k \to \infty$) and an FGM which is composed of these two materials. Tables 13-16 show that increasing the power law exponent and the nonlocal parameter causes a reduction in the critical buckling load for all types of boundary conditions. For example, for a constant power law exponent (i.e. $k = 0$) with $L/h = 20$, by changing the nonlocal parameter from $0\ \text{m}^2$ to $5\ \text{m}^2$, the nondimensional critical buckling load decreases by 86%, 45%, 93% and 96% for the pinned-pinned, fixed-free, fixed-pinned and fixed-fixed boundary conditions, respectively. Similar to the vibration behavior, for a fixed-fixed BC, the variation of the critical buckling load is most sensitive to the nonlocal parameter, while it is least sensitive for the fixed-free boundary condition. On the other hand, for a constant nonlocal parameter (i.e. $(ea_0)^2 = 0$), by changing power law exponent from 0 to ∞ , the nondimensional critical buckling load decreases by 81.6% for all four kinds of BCs (pinned-pinned, fixed-free, fixed-pinned and fixed-fixed) examined in this paper. Hence, the variation of the critical buckling load of an FGM nanobeam with nonlocal parameter is dependent on the boundary conditions while its variation with the power law exponent is the same for all types of BCs.

Table 13. Nondimensional critical buckling load of FGBs with varying nonlocal parameter for a pinned-pinned nanobeam.

| $(ea_0)^2[m^2]$ | $k = 0$ | $k = 0.1$ | $k = 0.2$ | $k = 0.5$ | $k = 1$ | $k = 2$ | $k = 5$ | $k = 10$ | $k \to \infty$ |
|---|---|---|---|---|---|---|---|---|---|
| $L/h = 20$ | | | | | | | | | |
| 0 | 53.2537 | 47.0464 | 43.3836 | 37.1323 | 32.2366 | 26.6616 | 18.9054 | 15.0478 | 9.8101 |
| 1 | 36.0154 | 34.1343 | 32.4946 | 28.6399 | 24.6432 | 19.7942 | 13.1382 | 9.9832 | 6.6345 |
| 2 | 18.0454 | 17.103 | 16.2815 | 14.3502 | 12.3476 | 9.9177 | 6.5828 | 5.002 | 3.3242 |
| 3 | 12.0386 | 11.4099 | 10.8619 | 9.5734 | 8.2374 | 6.6164 | 4.3916 | 3.337 | 2.2177 |
| 4 | 9.0321 | 8.5604 | 8.1492 | 7.1826 | 6.1802 | 4.964 | 3.2948 | 2.5036 | 1.6638 |
| 5 | 7.2272 | 6.8498 | 6.5208 | 5.7473 | 4.9452 | 3.972 | 2.6364 | 2.0033 | 1.3313 |

ACCEPTED MANUSCRIPT

| | | | | | | | | | |
|---|---|---|---|---|---|---|---|---|---|
| $L/h = 100$ | | | | | | | | | |
| 0 | 53.564 | 47.3014 | 43.6112 | 37.3214 | 32.4022 | 26.8019 | 19.0112 | 15.1368 | 9.8672 |
| 1 | 53.5111 | 47.2548 | 43.5682 | 37.2846 | 32.3702 | 7575.8937 | 5307.0541 | 3970.0525 | 9.8575 |
| 2 | 53.4584 | 47.2082 | 43.5252 | 37.2478 | 32.3383 | 4107.7234 | 2784.8898 | 2141.1301 | 9.8478 |
| 3 | 53.4056 | 47.1616 | 43.4823 | 37.2111 | 32.3064 | 2784.43 | 1887.7441 | 1451.3701 | 9.838 |
| 4 | 53.353 | 47.1151 | 43.4394 | 37.1744 | 32.2746 | 2105.9902 | 1427.7861 | 1097.7368 | 9.8283 |
| 5 | 53.3003 | 47.0687 | 43.3966 | 37.1377 | 32.2428 | 1693.388 | 1148.0566 | 882.67 | 9.8186 |

Table 14. Nondimensional critical buckling load of FGBs with varying nonlocal parameter for a fixed-free nanobeam.

| $(ea_0)^2[m^2]$ | $k = 0$ | $k = 0.1$ | $k = 0.2$ | $k = 0.5$ | $k = 1$ | $k = 2$ | $k = 5$ | $k = 10$ | $k \to \infty$ |
|---|---|---|---|---|---|---|---|---|---|
| $L/h = 20$ | | | | | | | | | |
| 0 | 13.374 | 11.8114 | 10.8903 | 9.32 | 8.0915 | 6.6928 | 4.747 | 3.7793 | 2.4637 |
| 1 | 13.2856 | 11.7337 | 10.8189 | 9.259 | 8.0385 | 19.7943 | 13.1382 | 9.9832 | 2.4474 |
| 2 | 13.184 | 11.6455 | 10.7381 | 9.1903 | 7.9787 | 9.9177 | 6.5828 | 5.002 | 2.4287 |
| 3 | 12.0384 | 11.4079 | 10.6452 | 9.1122 | 7.9107 | 6.6164 | 4.3916 | 3.337 | 2.2176 |
| 4 | 9.0321 | 8.5604 | 8.1492 | 7.1825 | 6.1802 | 4.964 | 3.2948 | 2.5036 | 1.6638 |
| 5 | 7.2272 | 6.8497 | 6.5207 | 5.7472 | 4.9452 | 3.972 | 2.6364 | 2.0033 | 1.3313 |
| $L/h = 100$ | | | | | | | | | |
| 0 | 13.3934 | 11.8274 | 10.9046 | 9.3318 | 8.1019 | 6.7016 | 4.7536 | 3.7849 | 2.4673 |
| 1 | 13.3901 | 11.8244 | 10.9019 | 9.3295 | 8.0999 | 7575.0446 | 5307.1717 | 3969.7013 | 2.4666 |
| 2 | 13.3868 | 11.8215 | 10.8992 | 9.3272 | 8.0979 | 4107.8208 | 2784.9602 | 2141.1795 | 2.466 |
| 3 | 13.3835 | 11.8186 | 10.8965 | 9.3249 | 8.0959 | 2784.4992 | 1887.7938 | 1451.405 | 2.4654 |
| 4 | 13.3802 | 11.8157 | 10.8938 | 9.3226 | 8.0939 | 2106.0438 | 1427.8245 | 1097.7637 | 2.4648 |
| 5 | 13.3769 | 11.8128 | 10.8911 | 9.3203 | 8.0919 | 1693.4318 | 1148.0879 | 882.6919 | 2.4642 |

Table 15. Nondimensional critical buckling load of FGBs with varying nonlocal parameter for a fixed-pinned nanobeam.

| $(ea_0)^2[m^2]$ | $k = 0$ | $k = 0.1$ | $k = 0.2$ | $k = 0.5$ | $k = 1$ | $k = 2$ | $k = 5$ | $k = 10$ | $k \to \infty$ |
|---|---|---|---|---|---|---|---|---|---|
| $L/h = 20$ | | | | | | | | | |
| 0 | 108.1294 | 95.6709 | 88.4238 | 76.2232 | 66.832 | 55.7539 | 39.2415 | 30.8956 | 19.9189 |
| 1 | 36.0158 | 34.1348 | 32.4952 | 28.6406 | 24.6437 | 19.7943 | 13.1382 | 9.9832 | 6.6345 |
| 2 | 18.0454 | 17.103 | 16.2815 | 14.3502 | 12.3476 | 9.9177 | 6.5828 | 5.002 | 3.3242 |
| 3 | 12.0386 | 11.4099 | 10.8619 | 9.5734 | 8.2374 | 6.6164 | 4.3916 | 3.337 | 2.2177 |
| 4 | 9.0321 | 8.5604 | 8.1492 | 7.1826 | 6.1802 | 4.964 | 3.2948 | 2.5036 | 1.6638 |
| 5 | 7.2272 | 6.8498 | 6.5208 | 5.7473 | 4.9452 | 3.972 | 2.6364 | 2.0033 | 1.3313 |
| $L/h = 100$ | | | | | | | | | |
| 0 | 109.5453 | 96.8373 | 89.4684 | 77.1004 | 67.6126 | 56.4247 | 39.7413 | 31.3087 | 20.1797 |
| 1 | 109.3243 | 96.6421 | 89.288 | 76.9449 | 67.4762 | 7575.0283 | 5307.1947 | 3969.6979 | 20.139 |
| 2 | 109.1039 | 96.4472 | 89.108 | 76.7898 | 67.3401 | 4107.8456 | 2784.9723 | 2141.1842 | 20.0984 |
| 3 | 108.8839 | 96.2528 | 88.9284 | 76.635 | 67.2044 | 2784.5161 | 1887.802 | 1451.4082 | 20.0579 |
| 4 | 108.6644 | 96.0589 | 88.7492 | 76.4806 | 67.0689 | 2106.0566 | 1427.8307 | 1097.7662 | 20.0174 |
| 5 | 108.4454 | 95.8653 | 88.5705 | 76.3266 | 66.9338 | 1693.442 | 1148.0928 | 882.6939 | 19.9771 |

Table 16. Nondimensional critical buckling load of FGBs with varying nonlocal parameter for a fixed-fixed nanobeam.

| $(ea_0)^2[m^2]$ | $k=0$ | $k=0.1$ | $k=0.2$ | $k=0.5$ | $k=1$ | $k=2$ | $k=5$ | $k=10$ | $k\to\infty$ |
|---|---|---|---|---|---|---|---|---|---|
| $L/h=20$ | | | | | | | | | |
| 0 | 209.2283 | 185.0674 | 170.7491 | 146.2145 | 126.9186 | 104.9293 | 74.3296 | 59.1058 | 38.5427 |
| 1 | 36.0158 | 34.1349 | 32.4953 | 28.6407 | 24.6438 | 19.7944 | 13.1383 | 9.9833 | 6.6345 |
| 2 | 18.0454 | 17.103 | 16.2815 | 14.3502 | 12.3476 | 9.9178 | 6.5828 | 5.002 | 3.3242 |
| 3 | 12.0386 | 11.4099 | 10.8619 | 9.5734 | 8.2374 | 6.6164 | 4.3916 | 3.337 | 2.2177 |
| 4 | 9.0321 | 8.5604 | 8.1492 | 7.1826 | 6.1802 | 4.9641 | 3.2948 | 2.5036 | 1.6638 |
| 5 | 7.2272 | 6.8498 | 6.5208 | 5.7473 | 4.9452 | 3.9721 | 2.6364 | 2.0033 | 1.3313 |
| $L/h=100$ | | | | | | | | | |
| 0 | 214.1002 | 189.0778 | 174.3307 | 149.1907 | 129.5258 | 107.1373 | 75.9916 | 60.5025 | 39.4401 |
| 1 | 213.2567 | 188.333 | 173.644 | 148.6031 | 129.0156 | 7574.7624 | 5307.525 | 3969.5846 | 39.2848 |
| 2 | 212.4167 | 187.5915 | 172.9604 | 148.0182 | 128.5078 | 4108.1133 | 2785.1718 | 2141.3276 | 39.13 |
| 3 | 211.5803 | 186.8533 | 172.28 | 147.436 | 128.0023 | 2784.7073 | 1887.9433 | 1451.5098 | 38.976 |
| 4 | 210.7474 | 186.1184 | 171.6027 | 146.8565 | 127.4992 | 2106.2049 | 1427.9399 | 1097.8447 | 38.8225 |
| 5 | 209.9181 | 185.3868 | 170.9285 | 146.2798 | 126.9984 | 1693.5631 | 1148.1817 | 882.7578 | 38.6697 |

To show the role of material distribution and size effects on the natural frequency and buckling load of nonlocal FG Timoshenko beams graphically, the following properties are considered, as given by Reddy [60]: $E_1 = 14.4\text{GPa}$, $E_2 = 1.44\text{GPa}$, $\rho_1 = 12.2 \times 10^3\ \text{kg/m}^3$, $\rho_2 = 1.22 \times 10^3\ \text{kg/m}^3$, $h = 17.6 \times 10^{-6}\text{m}$, $b = 2h$ and $L = 20h$. Also, it is assumed that $k_s G_i = E_i/3.16$, as given by [60] , where $i = 1, 2$ denotes the two different materials.

The effect of the nonlocal parameter and the power-law exponent $k$ on the natural frequencies of the pinned-pinned FG beam are examined with Timoshenko beam theory, and the first four natural frequencies are plotted in Fig. 4 for both local and nonlocal $[(ea_0)^2 = 0.1\ \text{nm}^2]$ cases and various power-law exponents. The prominent influence of through-thickness grading of the FGM on the natural frequencies is observed and consequently this fact could be employed to optimise the natural frequencies for design purposes. The influence of nonlocality is more significant when considering higher-order frequencies.

The effect of the nonlocal parameter and the power-law exponent $k$ on the critical buckling load of the pinned-pinned FG beam is examined with Timoshenko beams theory, and the first four buckling modes are plotted in Fig. 5 considering both local and nonlocal $[(ea_0)^2 = 0.1\ \text{nm}^2]$ cases and various power-law exponents. It is clear that, adjacent to the phase material 1, which has higher Young's modulus and density, the nondimensional critical bucking load changes quickly with varying exponent $k$, while the slope of the buckling load with respect to the exponent $k$, becomes almost zero as we approach material 2. Also, the effect of nonlocality will be more prominent when considering higher-order buckling modes.

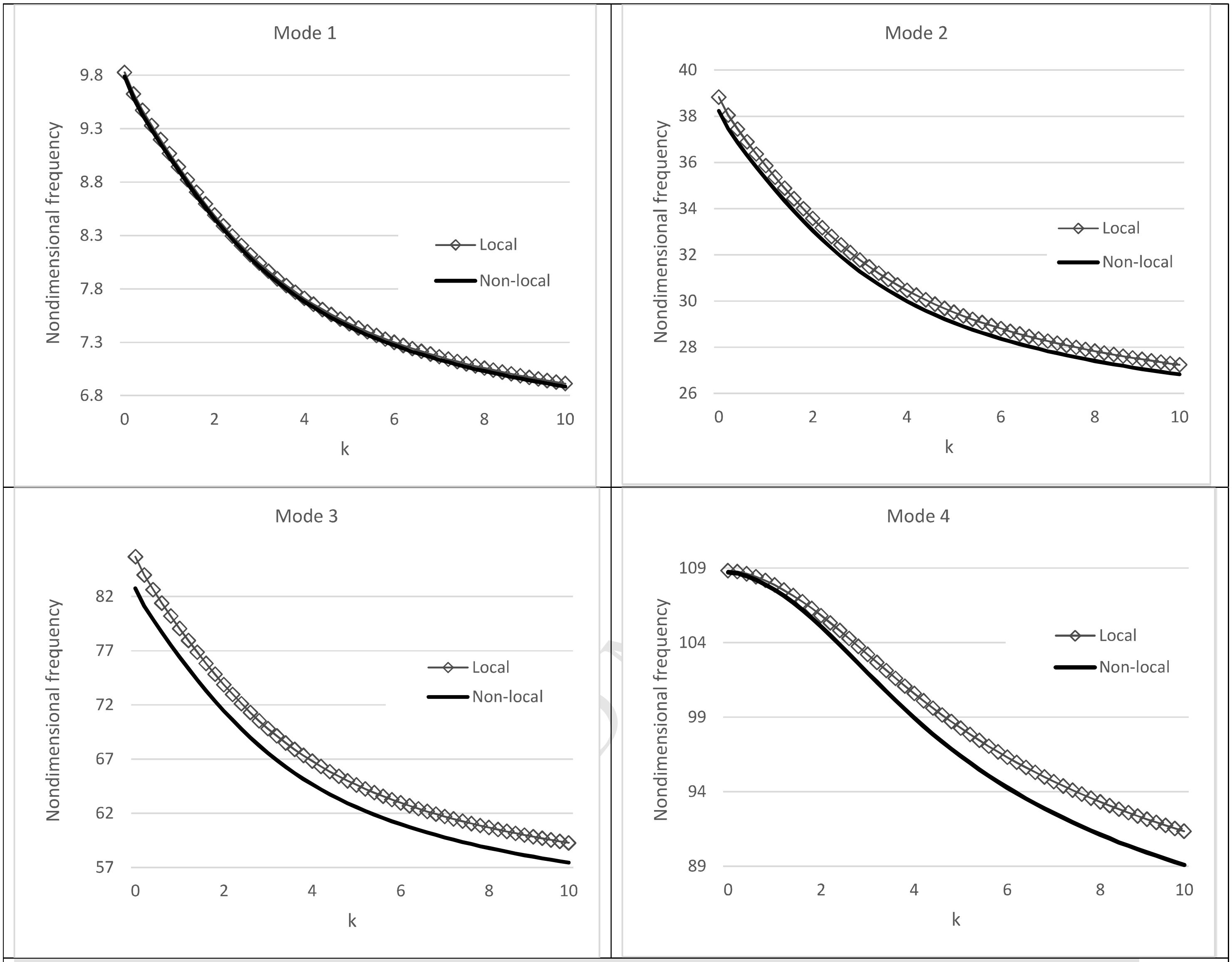


Figure 4. Effect of power-law index and nonlocality parameter on the first four nondimensional natural frequencies ($\hat{\omega} = \omega L^2\sqrt{\rho_2 A/E_2 I}$) of a simply supported FGM beam with $L/h = 100$.

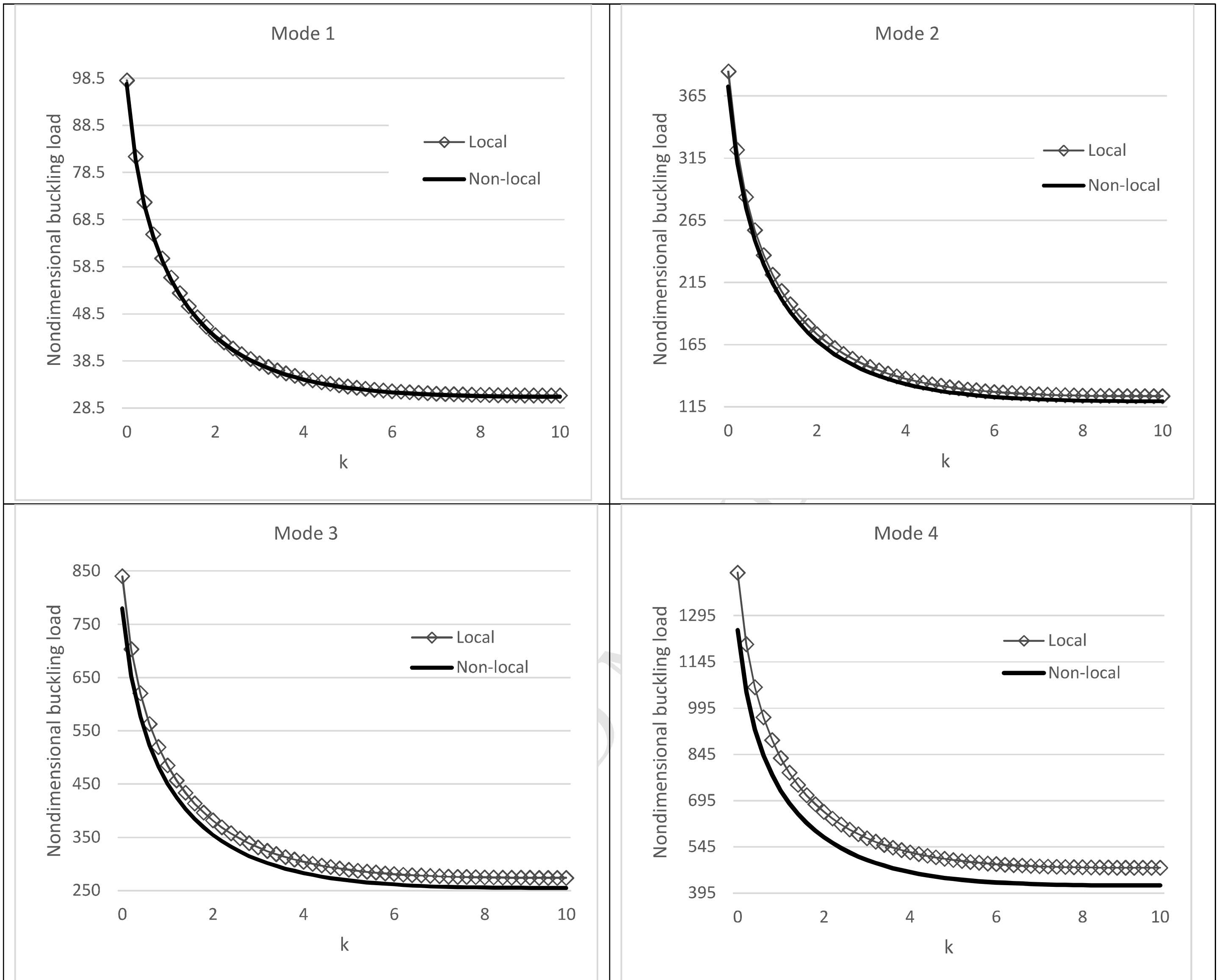


Figure 5. Effect of power-law index and nonlocality parameter on the first four nondimensional critical buckling loads ($\hat{P} = P\frac{12L^2}{E_2h^3}$) of a simply supported FGM beam with $L/h = 100$.

## 4. Conclusion

Based on the estimated neutral axis, a size-dependent 5-noded Timoshenko beam model is presented in the framework of strain-driven nonlocal elasticity theory for analyzing the free vibration and buckling of FGBs, with a through-thickness power-law variation. Both strain-driven and stress-driven formulations are discussed. By using Hamilton's principle, the governing equations and corresponding boundary conditions for FG Timoshenko beams are derived. The Timoshenko beam model includes a nonlocal parameter introduced to incorporate the importance of the nonlocal elastic stress field. Verification of the proposed model is performed in two stages including a validation procedure for an FG beam with different power law exponents and another one for a nonlocal homogeneous beam with various nonlocal parameters. Based on the results, the proposed model is able to accurately predict the fundamental natural frequencies and the critical buckling loads of functionally graded nanobeams for different BCs with a low computation effort. The significant effect of through-thickness material distribution of the FGM on the natural frequencies is seen. As a result, this fact can be used to optimise the natural frequencies for design purposes. Also, the effect of nonlocality is more prominent for higher-order frequencies and buckling loads.

# Appendix A

$$k_{aa} = \frac{L}{15}\begin{bmatrix} 2 & 1 & -1/2 \\ 1 & 8 & 1 \\ -1/2 & 1 & 2 \end{bmatrix}, \tag{A1}$$

$$k_{aa1} = \frac{1}{3L}\begin{bmatrix} 7 & -8 & 1 \\ -8 & 16 & -8 \\ 1 & -8 & 7 \end{bmatrix}, \tag{A2}$$

$$k_{aa2} = \frac{16}{L^3}\begin{bmatrix} 1 & -2 & 1 \\ -2 & 4 & -2 \\ 1 & -2 & 1 \end{bmatrix}, \tag{A3}$$

$$k_{bb} = \frac{L}{1680}\begin{bmatrix} 128 & 99 & -36 & 19 \\ 99 & 648 & -81 & -36 \\ -36 & -81 & 648 & 99 \\ 19 & -36 & 99 & 128 \end{bmatrix}, \tag{A4}$$

$$k_{bb1} = \frac{1}{40L}\begin{bmatrix} 148 & -189 & 54 & -13 \\ -189 & 432 & -297 & 54 \\ 54 & -297 & 432 & -189 \\ -13 & 54 & -189 & 148 \end{bmatrix}, \tag{A5}$$

$$k_{bb2} = \frac{81}{L^3}\begin{bmatrix} 1 & -5/2 & 2 & -1/2 \\ -5/2 & 7 & -13/2 & 2 \\ 2 & -13/2 & 7 & -5/2 \\ -1/2 & 2 & -5/2 & 1 \end{bmatrix}, \tag{A6}$$

$$k_{bc1} = \frac{1}{120}\begin{bmatrix} -83 & -44 & 7 \\ 99 & -108 & 9 \\ -9 & 108 & -99 \\ -7 & 44 & 83 \end{bmatrix}, \tag{A7}$$

$$k_{bc2} = \frac{1}{2L^2}\begin{bmatrix} -27 & 18 & -9 \\ 63 & -54 & 45 \\ -45 & 54 & -63 \\ 9 & -18 & 27 \end{bmatrix}, \quad \text{(A8)}$$

where $L$ is length of the beam element.

## Data Availability

All of the results given in the paper are simulated based on the proposed finite element model. The paper contains full details of the developed finite element and the geometry and material properties for the examples. Hence, there is no raw data, and data in the figures and tables maybe be reproduced by coding the described model.

## References

1. Johnson, K.L, Gidley, M.J, Bacic, A, Doblin, M. S. (2018). Cell wall biomechanics: a tractable challenge in manipulating plant cell walls 'fit for purpose'. Current Opinion in Biotechnology, 49, pp. 163-171.

2. Lebaschi, A. H, Deng, X. H, Camp, C. L, Zong, J, Cong, G. T, Carballo, C.B, Album, Z, Radeo, S. (2018), Biomechanical, histologic, and molecular evaluation of tendon healing in a new murine model of rotator cuff repair, Arthroscopy: The Journal of Arthroscopic & Related Surgery, 34(4), pp. 1173-1183.

3. Jandaghian, A. A, Rahmani, O. (2017), Size-dependent free vibration analysis of functionally graded piezoelectric plate subjected to thermo-electromechanical loading, Journal of Intelligent Material Systems and Structures, 28(20), pp. 3039–3053.

4. Şimşek, M., (2016). Nonlinear free vibration of a functionally graded nanobeam using nonlocal strain gradient theory and a novel Hamiltonian approach. International Journal of Engineering Science, 105, pp. 12-27.

5. Eringen, A.C., (1983). On differential equations of nonlocal elasticity and solutions of screw dislocation and surface waves. Journal of applied physics, 54(9), pp. 4703-4710.

6. Peddieson, J., Buchanan, G.R. and McNitt, R.P., 2003. Application of nonlocal continuum models to nanotechnology. International Journal of Engineering Science, 41(3-5), pp. 305-312.

7. Romano, G., Barretta, R., Diaco, M. and de Sciarra, F.M., 2017. Constitutive boundary conditions and paradoxes in nonlocal elastic nanobeams. International Journal of Mechanical Sciences, 121, pp. 151-156.

ACCEPTED MANUSCRIPT

8. Barretta, R., Čanadija, M., Feo, L., Luciano, R., de Sciarra, F.M. and Penna, R., 2018. Exact solutions of inflected functionally graded nano-beams in integral elasticity. Composites Part B: Engineering, 142, pp. 273-286.

9. Barretta, R., Diaco, M., Feo, L., Luciano, R., de Sciarra, F.M. and Penna, R., 2018. Stress-driven integral elastic theory for torsion of nano-beams. Mechanics Research Communications, 87, pp. 35-41.

10. Barretta, R., Čanađija, M., Luciano, R. and de Sciarra, F.M., 2018. Stress-driven modeling of nonlocal thermoelastic behavior of nanobeams. International Journal of Engineering Science, 126, pp. 53-67.

11. Challamel, N. and Wang, C.M., 2008. The small length scale effect for a non-local cantilever beam: a paradox solved. Nanotechnology, 19(34), paper 345703.

12. Li, C., Yao, L., Chen, W. and Li, S., 2015. Comments on nonlocal effects in nano-cantilever beams. International Journal of Engineering Science, 87, pp. 47-57.

13. Barretta, R., Feo, L., Luciano, R. and de Sciarra, F.M., 2016. Application of an enhanced version of the Eringen differential model to nanotechnology. Composites Part B: Engineering, 96, pp. 274-280.

14. Romano, G. and Barretta, R., 2017. Nonlocal elasticity in nanobeams: the stress-driven integral model. International Journal of Engineering Science, 115, pp. 14-27.

15. Romano, G., Luciano, R., Barretta, R. and Diaco, M., 2018. Nonlocal integral elasticity in nanostructures, mixtures, boundary effects and limit behaviours. Continuum Mechanics and Thermodynamics, 30(3), pp. 641-655.

16. Barretta, R., Faghidian, S.A. and Luciano, R., 2018. Longitudinal vibrations of nano-rods by stress-driven integral elasticity. Mechanics of Advanced Materials and Structures, pp. 1-9.

17. Barretta, R., Faghidian, S.A., Luciano, R., Medaglia, C.M. and Penna, R., 2018. Stress-driven two-phase integral elasticity for torsion of nano-beams. Composites Part B: Engineering, 145, pp. 62-69.

18. Barretta, R., Luciano, R., de Sciarra, F.M. and Ruta, G., 2018. Stress-driven nonlocal integral model for Timoshenko elastic nano-beams. European Journal of Mechanics-A/Solids, 72, pp. 275-286.

19. Barretta, R., Faghidian, S.A., Luciano, R., Medaglia, C.M. and Penna, R., 2018. Free vibrations of FG elastic Timoshenko nano-beams by strain gradient and stress-driven nonlocal models. Composites Part B: Engineering, 154, pp. 20-32.

20. Ouakad, H.M., El-Borgi, S., Mousavi, S.M. and Friswell, M.I., 2018, Static and dynamic response of CNT nanobeam using nonlocal strain and velocity gradient theory. Applied Mathematical Modeling, 62, pp. 207-222.

21. Friswell, M.I., Adhikari, S. and Lei, Y., 2007. Vibration analysis of beams with non local foundations using the finite element method. International Journal for Numerical Methods in Engineering, 71(11), pp. 1365-1386.

22. Phadikar, J.K. and Pradhan, S.C., 2010. Variational formulation and finite element analysis for nonlocal elastic nanobeams and nanoplates. Computational materials science, 49(3), pp. 492-499.

23. Murmu, T. and Adhikari, S., 2010. Nonlocal transverse vibration of double-nanobeam-systems. Journal of Applied Physics, 108(8), paper 083514.

24. Mustapha, K.B. and Zhong, Z.W., 2010. Free transverse vibration of an axially loaded non-prismatic single-walled carbon nanotube embedded in a two-parameter elastic medium. Computational Materials Science, 50(2), pp. 742-751.

25. Roque, C.M.C., Ferreira, A.J.M. and Reddy, J.N., 2011. Analysis of Timoshenko nanobeams with a nonlocal formulation and meshless method. International Journal of Engineering Science, 49(9), pp. 976-984.

26. Thai, H.T., 2012. A nonlocal beam theory for bending, buckling, and vibration of nanobeams. International Journal of Engineering Science, 52, pp. 56-64.

27. Thai, H.T. and Vo, T.P., 2012. A nonlocal sinusoidal shear deformation beam theory with application to bending, buckling, and vibration of nanobeams. International Journal of Engineering Science, 54, pp. 58-66.

28. Lei, Y., Adhikari, S. and Friswell, M.I., 2013. Vibration of nonlocal Kelvin–Voigt viscoelastic damped Timoshenko beams. International Journal of Engineering Science, 66, pp. 1-13.

29. Civalek, Ö. and Demir, C., 2016. A simple mathematical model of microtubules surrounded by an elastic matrix by nonlocal finite element method. Applied Mathematics and Computation, 289, pp. 335-352.

30. Kahya, V. and Turan, M., 2017. Finite element model for vibration and buckling of functionally graded beams based on the first-order shear deformation theory. Composites Part B: Engineering, 109, pp. 108-115.

31. Kahrobaiyan, M.H., Asghari, M., Rahaeifard, M. and Ahmadian, M.T., 2010. Investigation of the size-dependent dynamic characteristics of atomic force microscope microcantilevers based on the modified couple stress theory. International Journal of Engineering Science, 48(12), pp. 1985-1994.

32. Zhang, J. and Fu, Y., 2012. Pull-in analysis of electrically actuated viscoelastic microbeams based on a modified couple stress theory. Meccanica, 47(7), pp. 1649-1658.


ACCEPTED MANUSCRIPT

33. Shariat, B.S., Liu, Y. and Rio, G., 2013. Modelling and experimental investigation of geometrically graded NiTi shape memory alloys. Smart Materials and Structures, 22(2), paper 025030.

34. Eltaher, M.A., Emam, S.A. and Mahmoud, F.F., 2012. Free vibration analysis of functionally graded size-dependent nanobeams. Applied Mathematics and Computation, 218(14), pp. 7406-7420.

35. Uymaz, B., 2013. Forced vibration analysis of functionally graded beams using nonlocal elasticity. Composite Structures, 105, pp. 227-239.

36. Rahmani, O. and Pedram, O., 2014. Analysis and modeling the size effect on vibration of functionally graded nanobeams based on nonlocal Timoshenko beam theory. International Journal of Engineering Science, 77, pp. 55-70.

37. Nejad, M.Z. and Hadi, A., 2016. Non-local analysis of free vibration of bi-directional functionally graded Euler–Bernoulli nano-beams. International Journal of Engineering Science, 105, pp. 1-11.

38. Şimşek, M., 2014. Large amplitude free vibration of nanobeams with various boundary conditions based on the nonlocal elasticity theory. Composites Part B: Engineering, 56, pp. 621-628.

39. Niknam, H. and Aghdam, M.M., 2015. A semi analytical approach for large amplitude free vibration and buckling of nonlocal FG beams resting on elastic foundation. Composite Structures, 119, pp. 452-462.

40. El-Borgi, S., Fernandes, R. and Reddy, J.N., 2015. Non-local free and forced vibrations of graded nanobeams resting on a non-linear elastic foundation. International Journal of Non-Linear Mechanics, 77, pp. 348-363.

41. Thai, S., Thai, H.T., Vo, T.P. and Lee, S., 2018. Postbuckling analysis of functionally graded nanoplates based on nonlocal theory and isogeometric analysis. Composite Structures, 201, pp. 13-20.

42. Barretta, R., Fazelzadeh, S.A., Feo, L., Ghavanloo, E. and Luciano, R., 2018. Nonlocal inflected nano-beams: A stress-driven approach of bi-Helmholtz type. Composite Structures, 200, pp. 239-245.

43. Dastjerdi, S. and Akgöz, B., 2018. New static and dynamic analyses of macro and nano FGM plates using exact three-dimensional elasticity in thermal environment. Composite Structures, 192, pp. 626-641.

44. Eltaher, M.A., Emam, S.A. and Mahmoud, F.F., 2013. Static and stability analysis of nonlocal functionally graded nanobeams. Composite Structures, 96, pp. 82-88.

45. Barretta, R., Feo, L., Luciano, R., de Sciarra, F.M. and Penna, R., 2016. Functionally graded Timoshenko nanobeams: a novel nonlocal gradient formulation. Composites Part B: Engineering, 100, pp. 208-219.




ACCEPTED MANUSCRIPT

46. Čanađija, M., Barretta, R. and de Sciarra, F.M., 2016. On functionally graded Timoshenko nonisothermal nanobeams. Composite Structures, 135, pp. 286-296.

47. Barretta, R., 2013. On Cesàro-Volterra method in orthotropic Saint-Venant beam. Journal of Elasticity, 112(2), pp. 233-253.

48. Romano, G., Barretta, R. and Diaco, M., 2017. On nonlocal integral models for elastic nano-beams. International Journal of Mechanical Sciences, 131, pp. 490-499.

49. Romano, G. and Barretta, R., 2017. Stress-driven versus strain-driven nonlocal integral model for elastic nano-beams. Composites Part B, 114, pp. 184-188.

50. Li, L., Tang, H. and Hu, Y., 2018. The effect of thickness on the mechanics of nanobeams. International Journal of Engineering Science, 123, pp. 81-91.

51. Yuan, F.G. and Miller, R.E., 1990. A higher order finite element for laminated beams. Composite structures, 14(2), pp. 125-150.

52. Şimşek, M., 2010. Fundamental frequency analysis of functionally graded beams by using different higher-order beam theories. Nuclear Engineering and Design, 240(4), pp. 697-705.

53. Li, S.R. and Batra, R.C., 2013. Relations between buckling loads of functionally graded Timoshenko and homogeneous Euler–Bernoulli beams. Composite Structures, 95, pp. 5-9.

54. Nguyen, T.K., Nguyen, T.T.P., Vo, T.P. and Thai, H.T., 2015. Vibration and buckling analysis of functionally graded sandwich beams by a new higher-order shear deformation theory. Composites Part B: Engineering, 76, pp. 273-285.

55. Vo, T.P., Thai, H.T., Nguyen, T.K., Maheri, A. and Lee, J., 2014. Finite element model for vibration and buckling of functionally graded sandwich beams based on a refined shear deformation theory. Engineering Structures, 64, pp. 12-22.

56. Vo, T.P., Thai, H.T., Nguyen, T.K., Inam, F. and Lee, J., 2015. A quasi-3D theory for vibration and buckling of functionally graded sandwich beams. Composite Structures, 119, pp. 1-12.

57. Reddy, J.N., 2007. Nonlocal theories for bending, buckling and vibration of beams. International Journal of Engineering Science, 45(2-8), pp. 88-307.

58. Pradhan, S.C. and Phadikar, J.K., 2009. Bending, buckling and vibration analyses of nonhomogeneous nanotubes using GDQ and nonlocal elasticity theory. Structural Engineering and Mechanics, 33(2), pp. 193-213.

59. Aria, A.I. and Biglari, H., 2018. Computational vibration and buckling analysis of microtubule bundles based on nonlocal strain gradient theory. Applied Mathematics and Computation, 321, pp. 313-332.

60. Reddy, J.N., 2011. Microstructure-dependent couple stress theories of functionally graded beams. Journal of the Mechanics and Physics of Solids, 59(11), pp. 2382-2399.

ACCEPTED MANUSCRIPT